# ROBUSTIFIED $H_2$-CONTROL OF A SYSTEM WITH LARGE STATE DIMENSION

L. Ravanbod*†, D. Noll*, J.-P. Raymond*, and J.-M. Buchot*

Abstract. We consider the design of an output feedback controller for a large scale system like the linearized Navier-Stokes equation. We design an observer-based controller for a reduced system that achieves a compromise between concurring performance and robustness specifications. This controller is then pulled back to the large scale system such that closed-loop stability is preserved, and such that the trade-off between the $H_2$- and $H_\infty$-criteria achieved in reduced space is preserved. The procedure is tested on a simulated fluid flow study.

**Key words:** Robustified $H_2$-control · Navier-Stokes equation · output feedback control · reduced-order system · performance versus robustness · structured control law.

## 1. Introduction

Robust feedback control of systems with large state dimension like the linearized Navier-Stokes equation hinges on system reduction techniques. Bringing the system down to a moderate size allows to apply sophisticated optimization-based robust controller synthesis tools, which achieve a compromise between performance and robustness specifications. The controller so obtained is then pulled back to the large dimension, and one hopes that it still achieves a similar compromise in the large scale space.

In order to justify this approach theoretically, one first of all has to prove that the pull back procedure preserves stability in closed loop (Raymond and Thevenet, 2010; Thevenet, 2009). The more intriguing question is then whether pull back also preserves the trade-off between performance and robustness specifications (Bernstein et al. 1989; Stein and Athans, 1987; Doyle et al. 1982) achieved in reduced space. Namely, stability is rarely the main issue in practical control applications. The real difficulties surface when it comes to assuring good performance and robustness in the presence of the inevitable system uncertainty.

In this work we present a new technique which allows to achieve such a compromise between performance and robustness within the framework of observer-based controllers. This may seem surprising at first, as $H_2$- or LQG control is known to be fragile in the presence of system uncertainty and finite energy external perturbations, which is why it has been supplanted by robust control techniques in practice (Lauga and Bewley, 2004; Farag and Werner, 2002; Lauga and Bewley, 2002; Feron, 1997; Bernstein et al. 1989; Packard and Doyle, 1987; Doyle and Stein, 1979). Since our reduction and pull-back technique makes it necessary to continue to use observer-based controllers, we have to robustify them, and this is where the use of optimization techniques becomes inevitable. In consequence, practically useful observer-based controllers can no longer be computed by solving algebraic Riccati (ARE) equations. In particular, we cannot benefit from recent progress (Benner et al. 2004) obtained in solving large-scale AREs.

*Date*: May 20, 2016.

*All authors are with Université Paul Sabatier, Institut de Mathématiques, 118 route de Narbonne, 31062 Toulouse, France.

†Corresponding author.

Roughly our approach can be described as follows. We show how a standard $H_2$-performance channel can be traded against an $H_\infty$-robustness specification in reduced space such that the resulting mixed $H_2/H_\infty$-controller achieves a satisfactory compromise between performance and robustness in reduced space. We then show that the mixed controller still achieves a good compromise when pulled back to the large system. This is a consequence of the fact that the projection/pull-back operation preserves local optimality if the $H_2$ and $H_\infty$ channels are suitably re-normed in the large scale space.

The structure of the paper is as follows. In section 2 we recall the PEVA system reduction technique, which is later used in open and in closed loop. Section 4 presents our line of action and gives the main result. In particular, the algorithm proposed in that section realizes the trade-off between performance and robustness specifications. In section 5 we briefly recall the choice of performance and robustness filters for the LQG case. Section 6 gives the proofs of the principal results. In section 7 we apply our theory to control the linearized Navier-Stokes equation, where the full order descriptor system after discretization features near 41000 states.

## 2. Review of the algorithm for partial eigenvalue assignment

The algorithm for partial eigenvalue assignment (PEVA) is a classical tool for system reduction (Datta, 2004), which we briefly recall here, as we shall need it in the sequel. Consider a linear system

$$(\mathcal{S}):\quad \begin{cases} \dot{\mathbf{x}} = \mathcal{A}\mathbf{x} + \mathcal{B}u \\ y = \mathcal{C}\mathbf{x} \end{cases} \tag{1}$$

where $\mathcal{A} \in \mathbb{R}^{n\times n}$, $\mathcal{B} \in \mathbb{R}^{n\times m}$ and $\mathcal{C} \in \mathbb{R}^{p\times n}$. We assume that the state dimension $n$ is exceedingly large, while $p, m$ are rather of moderate size. We adopt the convention that any matrix which has at least one large dimension (row or column) is represented by a non usual Latin symbol, for example: $\mathcal{A}, \mathcal{B}, \mathsf{A}, \mathsf{B}, \dots$, while small matrices have the usual Latin symbols $A, B, \dots$. Similarly, vectors with large state dimension have symbols like $\mathbf{x}, \widehat{\mathbf{x}}$, etc. while small dimensions are denoted as $x, \hat{x}$ as usual. Assuming $\mathcal{A}$ diagonalizable, we let $\mathcal{E}$ and $\mathcal{F}$ be bases of right and left eigenvectors of $\mathcal{A}$, that is

$$\mathcal{A}\mathcal{E} = \mathcal{E}\Lambda, \quad \text{and} \quad \mathcal{A}^T\mathcal{F} = \mathcal{F}\Lambda^*,$$

where $\Lambda = \mathrm{diag}(\lambda_1, ..., \lambda_n)$ are the eigenvalues of $\mathcal{A}$. Now we divide the set $I = \{1, \dots, n\}$ into two disjoint parts, $I_s$ and $I_u$ with $|I_s| = n_s$, $|I_u| = n_u$, $n_s + n_u = n$, where it is assumed that unstable eigenvalues belong to $I_u$, that is

$$\{i : \mathrm{Re}(\lambda_i) \geq 0\} \subset I_u.$$

That is, we oblige all unstable modes to belong to $I_u$, but allow some of the stable ones in $I_u$, too. Nonetheless, in slight *abus de langue*, we call $\lambda_i$ with $i \in I_u$ the unstable open-loop modes, and $I_s$ the stable modes. The set $I_u$ does in fact include those open-loop modes which we wish to (or have to) control by feedback, whereas the modes in $I_s$ are considered extremely fast and irrelevant for feedback.

Now let $\mathcal{E}_u$ be the right eigenvectors in $\mathcal{E}$ associated with $\lambda_i$, $i \in I_u$, $\mathcal{E}_s$ those in $\mathcal{I}_s$, and similarly, $\mathcal{F}_u$ the left eigenvectors associated with $\lambda_i$ in $I_u$, $\mathcal{F}_s$ those in $\mathcal{I}_s$. By orthogonality we have

$$\mathcal{F}_s^T\mathcal{E}_u = 0_{n_s\times n_u}, \quad \mathcal{F}_u^T\mathcal{E}_s = 0_{n_u\times n_s}. \tag{2}$$

In addition, we may also arrange for $\mathcal{E}_u, \mathcal{E}_s, \mathcal{F}_u, \mathcal{F}_s$ to be real matrices and to be scaled to satisfy

$$\mathcal{F}_s^T\mathcal{E}_s = \mathcal{I}_{n-n_u}, \quad \mathcal{F}_u^T\mathcal{E}_u = I_{n_u}. \tag{3}$$

To arrange this we first replace $[\mathcal{F}_u^{(i)},\, \mathcal{F}_u^{(i+1)}]$ and $[\mathcal{E}_u^{(i)},\, \mathcal{E}_u^{(i+1)}]$ associated with a pair of complex conjugate eigenvalues with indexes $i$ and $i+1$, by

$$[\mathcal{F}_u^{(i)},\, \mathcal{F}_u^{(i+1)}]G^* \text{ and } [\mathcal{E}_u^{(i)},\, \mathcal{E}_u^{(i+1)}]G^*,$$

where $G = \frac{1}{\sqrt{2}}\begin{pmatrix} 1 & 1 \\ j & -j \end{pmatrix}$, $j^2 = -1$. Then we normalize them.

Using (2), (3), we can now decompose the state $\mathbf{x}$ of the large scale system (1) as $\mathbf{x} = \mathcal{E}_u x_u + \mathcal{E}_s \mathbf{x}_s$, where $x_u, \mathbf{x}_s$ are the states of the following two subsystems, called the unstable and the stable subsystem:

$$(S_u): \quad \begin{cases} \dot{x}_u = A_u x_u + B_u u \\ y_u = C_u x_u \end{cases}, \quad (\mathcal{S}_s): \quad \begin{cases} \dot{\mathbf{x}}_s = \mathcal{A}_s \mathbf{x}_s + \mathcal{B}_s u \\ y_s = \mathcal{C}_s \mathbf{x}_s \end{cases} \tag{4}$$

where:

$$\begin{aligned} A_u &= \mathcal{F}_u^T \mathcal{A} \mathcal{E}_u = \Lambda_u,\ B_u = \mathcal{F}_u^T \mathcal{B},\ C_u = \mathcal{C}\mathcal{E}_u, \\ \mathcal{A}_s &= \mathcal{F}_s^T \mathcal{A} \mathcal{E}_s = \Lambda_s,\ \mathcal{B}_s = \mathcal{F}_s^T \mathcal{B},\ \mathcal{C}_s = \mathcal{C}\mathcal{E}_s. \end{aligned} \tag{5}$$

Here $\Lambda_u$ are the unstable eigenvalues, $\Lambda_s$ the stable eigenvalues of $\mathcal{A}$. The equations of the original system $(\mathcal{S})$, given in (1), can be obtained back from the equations of the unstable system $(S_u)$ and stable system $(\mathcal{S}_s)$ given in (4), bearing in mind that $\mathbf{x} = \mathcal{E}[x_u,\ \mathbf{x}_s]^T$ and $y = y_u + y_s$. In other words, the procedure presented so far is loss-less.

## 3. Problem statement

In order to control the large scale system $(\mathcal{S})$ appropriately, we have to embed it into a plant $\mathcal{P}$ by adding performance and robustness channels. We decide to assess the performance by a weighted $H_2$-norm, while a robustness criterion based on a weighted $H_\infty$-norm is added. Altogether, this leads to the following large scale plant

$$\mathcal{P}: \begin{cases} \begin{array}{rlllll} \dot{\mathbf{x}} & = \mathcal{A}\mathbf{x} & & +\mathcal{B}_2 w_2 & +\mathcal{B}_\infty w_\infty & +\mathcal{B}u \\ \dot{x}_2 & = \mathcal{A}_2\mathbf{x} + A_{22}x_2 & & +B_{22}w_2 & & +B_{2u}u \\ \dot{x}_\infty & = \mathcal{A}_\infty \mathbf{x} & +A_{\infty\infty}x_\infty & & +B_{\infty\infty}w_\infty & +B_{\infty u}u \\ z_2 & = \mathcal{C}_2\mathbf{x} + C_{22}x_2 & & & & +D_{2u}u \\ z_\infty & = \mathcal{C}_\infty \mathbf{x} & +C_{\infty\infty}x_\infty & & +D_{\infty\infty}w_\infty & +D_{\infty u}u \\ y & = \mathcal{C}\mathbf{x} & & +D_{y2}w_2 & +D_{y\infty}w_\infty, & \end{array} \end{cases} \tag{6}$$

where $w_\infty$ is bounded energy perturbations, $w_2$ is a white noise source, $\mathbf{x}$ is the system state with large dimension $n$, while $x_2$, $x_\infty$ represent the states of the stable filters used for frequency weighting. Here $z_2$ and $z_\infty$ are the controlled outputs of these filters. With the exception of $\mathcal{A}$, $\mathcal{B}$ and $\mathcal{C}$, all other matrices are specified once performance and robustness channels are chosen.

**Remark 1.** Our notation highlights plant data involving the large state dimension by using calligraphic symbols, while the small dimension is indicated by using roman symbols. Note that $\mathcal{B}_2, \mathcal{B}_\infty$ and also $\mathcal{A}_2, \mathcal{A}_\infty$ and $\mathcal{C}_2, \mathcal{C}_\infty$ have at least one large dimension, but these matrices are under our control, so we can arrange them to be sparse.

In the sequel, we make the following assumption:

$$(\mathcal{A}, \mathcal{B}) \text{ is stabilizable, } (\mathcal{A}, \mathcal{C}) \text{ is detectable, } \mathcal{A} \text{ is diagonalizable.}$$

We also work under the informal hypothesis that $n_u \ll n$, as otherwise our reduction technique will not kick in. Similarly, it is realistic to assume that $\dim y \ll \dim \mathbf{x}$. Naturally, we also assume that $\mathcal{A}_2, \mathcal{A}_\infty$ are stable. Our goal is to design a dynamic output feedback controller of observer structure

$$u(s) = \mathcal{K}(s)y(s) = -\mathcal{K}_c\left(sI - (\mathcal{A} - \mathcal{B}\mathcal{K}_c - \mathcal{K}_f^T\mathcal{C})\right)^{-1}\mathcal{K}_f^T y(s) \tag{7}$$

for the large scale system $(\mathcal{S})$, such that the following design specifications are satisfied:

(i) $\mathcal{K}$ stabilizes $(\mathcal{S})$ in closed loop.
(ii) The controller has good performance in the sense that a suitable frequency weighted $H_2$-norm of the closed-loop performance channel $w_2 \to z_2$ is small.
(iii) The controller has acceptable robustness in the sense that a suitable frequency weighted $H_\infty$-norm of the closed-loop robustness channel $w_\infty \to z_\infty$ is small.
(iv) The controller $\mathcal{K}$ should be practically computable. That rules out the nominal mixed $H_2/H_\infty$ controller, where the dimensions of $\mathcal{K}_f$ and $\mathcal{K}_c$ satisfying Riccati equations would be exceedingly large. The controller and filter gains should be computed using a reduced-order plant.

For the following, let us introduce the notation $\theta = (\mathcal{K}_c, \mathcal{K}_f)$ for a vector $\theta$ gathering all unknown controller and observer gains of (7), and let the corresponding observer-based controller in (7) be $\mathcal{K}(\theta)$. Moreover, let $T_{z_2w_2}(s,\theta)$ be the closed-loop transfer function $w_2 \to z_2$ of the large scale plant $\mathcal{P}$ when controller $\mathcal{K}(\theta)$ is used, and similarly $T_{z_\infty w_\infty}(s,\theta)$ the closed-loop channel $w_\infty \to z_\infty$ using $\mathcal{K}(\theta)$ in feedback with $\mathcal{P}$. Then we wish to solve an optimization problem of the form

$$\begin{array}{ll} \text{minimize} & \mathcal{P}(\theta) = \|F_1^{(2)}T_{z_2w_2}(\cdot,\theta)F_2^{(2)} + F_3^{(2)}\|_2 \\ \text{subject to} & \mathcal{R}(\theta) = \|F_1^{(\infty)}T_{z_\infty w_\infty}(\cdot,\theta)F_2^{(\infty)} + F_3^{(\infty)}\|_\infty \leq r \\ & \theta = (\mathcal{K}_c, \mathcal{K}_f) \text{ closed-loop stabilizing} \end{array} \tag{8}$$

in the large scale space. Here $\mathcal{P}(\theta)$ is called the performance criterion, $\mathcal{R}(\theta)$ the robustness criterion, and $r$ is a suitable robustness threshold. The frequency filters $F_i^{(k)}(s)$ are independent of the design parameter $\theta$. Note that the matrix dimensions of $T_{z_2w_2}$ and $T_{z_\infty w_\infty}$ are small, but large matrices are required to compute them, so they are not readily available for synthesis.

It is clear that unless simplifying manipulations are made, (8) will present major numerical difficulties due to the size of the matrices involved in computing the transfer function $T_{zw}$ in the large scale space. In the next section we show how the PEVA reduction technique may be applied to the ambitious program (8) to obtain a version in reduced order space which is amenable to computations in such a way that the results remain meaningful in the large dimension.

## 4. Course of action

In this section we present our main idea to control the large scale system $(\mathcal{S})$ in (1). We focus on the unstable system $(S_u)$, which by our working hypothesis has significantly reduced order $\dim(x_u) \ll \dim(\mathbf{x})$. We design a controller $K$ for $(S_u)$, which we then lift, or *pull back* to a controller $\mathcal{K}$ in the original system $(\mathcal{S})$. The challenge is to do this in such a way that the lifted controller has reasonable properties with regard to the performance robustness trade-off in program (8).

Extending the PEVA reduction technique to the plant $\mathcal{P}$ leads to the following reduced-order plant.

$$(9)\qquad P_u : \begin{cases} \dot{x}_u &= A_u x_u & & +B_2 w_2 & +B_\infty w_\infty & +B_u u \\ \dot{x}_2 &= A_2 x_u + A_{22} x_2 & & +B_{22} w_2 & & +B_{2u} u \\ \dot{x}_\infty &= A_\infty x_u & +A_{\infty\infty} x_\infty & & +B_{\infty\infty} w_\infty & +B_{\infty u} u \\ z_{2_u} &= C_2 x_u + C_{22} x_2 & & & & +D_{2u} u \\ z_{\infty_u} &= C_\infty x_u & +C_{\infty\infty} x_\infty & & +D_{\infty\infty} w_\infty & +D_{\infty u} u \\ y_u &= C_u x_u & & +D_{y2} w_2 & +D_{y\infty} w_\infty, & \end{cases}$$

where $x_u$ represents the state of the unstable reduced plant $P_u$, $x_2$ is the state of a $H_2$-performance filter for the channel $w_2 \to z_{2_u}$, $x_\infty$ is the state of the $H_\infty$-robustness channel $w_\infty \to z_{\infty_u}$, and where it is assumed as in $\mathcal{P}$ that the original system dynamics do not feature the states of the filters. In particular, we have

$$(10)\qquad \begin{array}{l} A_u = \mathcal{F}_u^T \mathcal{A} \mathcal{E}_u,\ A_2 = \mathcal{A}_2 \mathcal{E}_u,\ A_\infty = \mathcal{A}_\infty \mathcal{E}_u,\ B_u = \mathcal{F}_u^T \mathcal{B},\ B_2 = \mathcal{F}_u^T \mathcal{B}_2,\ B_\infty = \mathcal{F}_u^T \mathcal{B}_\infty, \\ C_2 = \mathcal{C}_2 \mathcal{E}_u,\ C_\infty = \mathcal{C}_\infty \mathcal{E}_u,\ C_u = \mathcal{C} \mathcal{E}_u. \end{array}$$

Note that the matrices with roman symbols in $\mathcal{P}$ re-appear in $P_u$ without changes. Note also that there is no plant $\mathcal{P}_s$ defined for the stable system $\mathcal{S}_s$, as our approach leaves this subsystem uncontrolled.

**Lemma 1.** *In the unstable reduced system $(A_u, B_u)$ is stabilizable and $(A_u, C_u)$ is detectable.*

*Proof.* Stabilizability of $(A_u, B_u)$ follows from PEVA algorithm. It is well known that

$$(\mathcal{A}, \mathcal{C}) \text{ detectable } \Leftrightarrow (\mathcal{A}^T, \mathcal{C}^T) \text{ stabilizable.}$$

Because $\mathcal{A}$ diagonalizable $\Leftrightarrow$ $\mathcal{A}^T$ diagonalizable, then

$$(\mathcal{A}^T, \mathcal{C}^T) \text{ stabilizable } \Leftrightarrow (A_u^T, C_u^T) \text{ stabilizable } \Leftrightarrow (A_u, C_u) \text{ detectable.}$$

□

As a consequence of this lemma, and since the state-dimension of $P_u$ is reduced, we can now compute observer-based controllers which stabilize $(S_u)$ in closed loop. Let us introduce the notation

$$(11)\qquad u(s) = K(s, \vartheta) y_u(s) = -K_c \left( sI - (A_u - B_u K_c - K_f^T C_u) \right)^{-1} K_f^T y_u(s)$$

where $\vartheta = (K_c, K_f)$ now gathers the gains of the reduced-order observer-based controller $K = K(\vartheta)$. We introduce the following optimization program for the small dimension $n_u$:

$$(12)\qquad \begin{array}{ll} \text{minimize} & P(\vartheta) = \|T_{z_{2_u} w_2}(\cdot, \vartheta)\|_2 \\ \text{subject to} & R(\vartheta) = \|T_{z_{\infty_u} w_\infty}(\cdot, \vartheta)\|_\infty \leq r \\ & \vartheta = (K_c, K_f) \text{ stabilizes } (S_u) \text{ in closed loop} \end{array}$$

where $P(\vartheta)$, $R(\vartheta)$ are now the performance and robustness criteria in reduced space. Suppose we have computed a locally optimal solution $\vartheta^* = (K_c^*, K_f^*)$ of (12), then we have to pull $K(\vartheta^*)$ back to the large dimension. Let us explain how this is arranged. We simply put

$$(13)\qquad \mathcal{K}_c = K_c \mathcal{F}_u^T, \quad \mathcal{K}_f = K_f \mathcal{E}_u^T,$$

so that $\theta = (K_c \mathcal{F}_u^T, K_f \mathcal{E}_u^T) = \theta(\vartheta)$. We call $\vartheta \to \theta$ respectively $K(\vartheta) \to \mathcal{K}(\theta)$ the pull back operator. We shall also say that $\mathcal{K}(\theta)$ is pulled back from $K(\vartheta)$.

**Remark 2.** The controller $(\mathcal{K}_f, \mathcal{K}_c)$ acts in the original large-dimensional space ($\mathcal{K}_f \in \mathcal{R}^{p\times n}$, $\mathcal{K}_c \in \mathcal{R}^{m\times n}$). The fact that it is a pull back from the controller $(K_f, K_c)$ designed in the low-dimensional space via program (12) is owed to the fact that solving optimization program (8) in dimension $n \times (m+p)$ is not possible.

The principal question which will keep us occupied now is in which way the good properties of $K(\vartheta^*)$, the solution of (12), are preserved in (8) when we pull it back to $\mathcal{K}(\theta^*)$. Our first result is a direct consequence of the PEVA procedure. We have the following well-known

**Proposition 2.** *Suppose the observer-based controller $K(\vartheta)$ stabilizes the reduced system $(S_u)$ in closed-loop. Then its pull back $\mathcal{K}(\theta)$ stabilizes the large dimensional system $(\mathcal{S})$ in closed-loop.*

*Proof.* This is shown in section 6. □

The following is more interesting and ultimately justifies our method.

**Theorem 3.** *Given the performance and robustness channels $T_{z_{2u}w_2}$ and $T_{z_{\infty u}w_\infty}$ in* (12)*, one can choose frequency filters $F_i^{(k)}$ (independent of $\theta$ and $\vartheta$) in large scale space such that $K(\vartheta^*)$ is a local minimum of the reduced-order mixed $H_2/H_\infty$ optimization program* (12) *with robustness threshold $r$, if and only if its pull back $\mathcal{K}(\theta^*)$ is a local minimum of* (8) *with the same $r$ where the admissible controllers are the pull back controllers.*

*Proof.* This theorem will also be proved in section 6. □

The following algorithm, inspired by (Ravanbod et al. 2012), is at the core of our trade-off approach.

**Algorithm 1 .**Trade-off between robustness and performance

1: **Initialization.** Divide the eigenvalues $\Lambda$ of $\mathcal{A}$ into two parts $\Lambda_u, \Lambda_s$ such that $\Lambda_u$ contains all unstable eigenvalues. Make sure that $\dim(\Lambda_u) \ll \dim(\Lambda_s)$. Compute the corresponding $\mathcal{E}_u, \mathcal{F}_u$.

2: **Define channels**. Identify suitable performance and robustness specifications $w_2 \to z_{2_u}$ and $w_\infty \to z_{\infty_u}$ by defining suitable filters. Compute plant $P_u$.

3: **Calibrate performance**. Compute best possible performance $p_\downarrow$ by solving the $H_2$-optimization program

$$\begin{array}{ll} \text{minimize} & \|T_{z_{2_u} w_2}(\vartheta)\|_2 \\ \text{subject to} & K(\vartheta) \text{ closed-loop stabilizing} \end{array}$$

The optimal $H_2$ controller $K(\vartheta_2)$ gives $p_\downarrow = \|T_{z_{2_u} w_2}(\vartheta_2)\|_2$. Its robustness is $r^\uparrow = \|T_{z_{\infty_u} w_\infty}(\vartheta_2)\|_\infty$. If the nominal $H_2$-controller is considered sufficiently robust, i.e., if $r^\uparrow$ is not too large, then pull the controller back to $\mathcal{K}(\theta_2)$ and quit. Otherwise continue.

4: **Calibrate robustness**. Compute optimal robustness $r_\downarrow$ by solving the structured $H_\infty$-program

$$\begin{array}{ll} \text{minimize} & \|T_{z_{\infty_u} w_\infty}(\vartheta)\|_\infty \\ \text{subject to} & K(\vartheta) \text{ closed-loop stabilizing} \end{array}$$

initialized by $K(\vartheta_2)$. The solution is $K(\vartheta_\infty)$ and satisfies $r_\downarrow = \|T_{z_{\infty_u} w_\infty}(\vartheta)_\infty)\|_\infty \ll r^\uparrow$. The performance of $K(\vartheta_\infty)$ is $p^\uparrow = \|T_{z_{2_u} w_2}(\vartheta_\infty)\|_2 \gg p_\downarrow$.

5: **Mixed synthesis**. Choose $r$ with $r_\downarrow < r < r^\uparrow$ and solve the mixed $H_2/H_\infty$-program

$$\begin{array}{ll} \text{minimize} & \|T_{z_{2_u} w_2}(\cdot, \vartheta)\|_2 \\ \text{subject to} & \|T_{z_{\infty_u} w_\infty}(\cdot, \vartheta)\|_\infty \leq r \\ & K(\vartheta) \text{ closed-loop stabilizing} \end{array}$$

initialized by $K(\vartheta_\infty)$. The solution is $\vartheta^*$.

6: **Evaluate performance**. If performance $p^* = \|T_{z_{2_u} w_2}(\vartheta^*)\|_2$ is satisfactory, then $\vartheta_{2/\infty} = \vartheta^*$ and pull controller back to obtain $\mathcal{K}(\theta^*)$ and quit. If performance $p^*$ is too large then relax robustness constraint by increasing $r \in (r_\downarrow, r^\uparrow)$ and go back to step 4.

**Remark 3.** The rationale of Algorithm 1 can be summarized as follows. In step 2 we choose a nominal performance channel, and a robustness channel with which we assess the robustness of the design. Our choice of the robustness channel may be guided by (Zhou and Doyle, 1998; Doyle et al., 1982), where a list of robustness specifications suited for various types of uncertainty is given. The more is know about the type of uncertainty, the better this channel can be adapted.

If the nominal controller is not sufficiently robust with respect to the chosen channel, then our procedure in steps 3 to 6 sets in. As a result, we can always enhance robustness, while keeping the performance of the mixed controller $\vartheta^*$ close to the nominal performance of $\vartheta_2$.

Note that in Algorithm 1 we do *not* question the choice of the $H_2$ performance channel itself. We enhance robustness while maintaining the original performance objective. Notwithstanding, there are also various heuristic procedures, where one modifies the nominal performance in order to enhance robustness. A prominent example is the LQG/LTR procedure, where e.g. the noise level in the output is artificially increased in order to robustify the design. For a discussion see (Ravanbod et al. 2012).

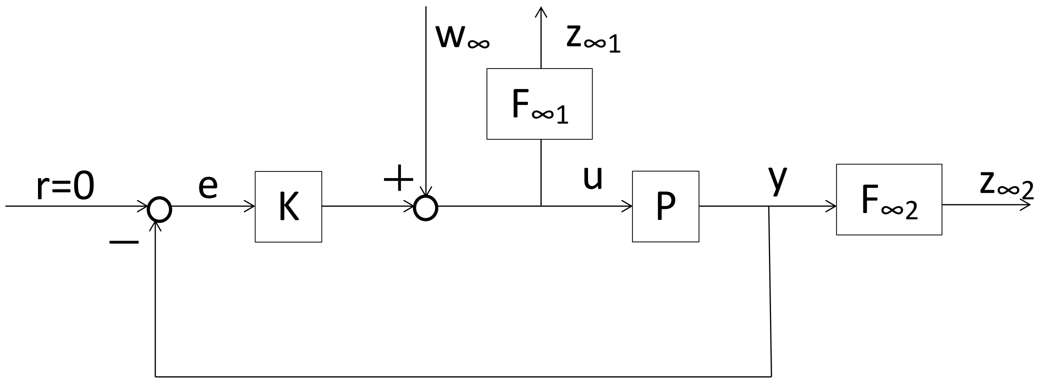


Figure 1. Feedback configuration with high-pass filter $F_{\infty 1}$ and low-pass filter $F_{\infty 2}$. The objectives are tracking of the steady-state $r = 0$ and attenuating finite energy external process noise $w_\infty$.

The fact that LQG- and $H_2$-controllers often require this posterior robustification became apparent to the control community in the late 1970s and 1980s. The phenomenon is not related to the state dimension of the system. We refer to (Bernstein and Haddad, 1989; Doyle and Stein, 1979) for a discussion.

## 5. Specific case of an LQG controller

It is well known that LQG control can be considered a special case of $H_2$ optimal control. In our numerical experiment we will indeed apply our mixed $H_2/H_\infty$-approach to compute a robustified version of the LQG controller. Recall that in LQG the $H_2$ performance channel in (9) is set-up as follows:

$A$). We consider following system

$$\begin{cases} \dot{x}_u = A_u x_u + B_u u + B_w w \\ y_u = C_u x_u + v \end{cases} .$$

The covariance matrices of process noise, $w$, and measurement noise, $v$, are called respectively, $W$ and $V$.

$B$). We choose weighting matrices $R_y$ and $R_u$ in the quadratic performance criterion

$$J_u := \lim_{T\to\infty} \frac{1}{T} \int_0^T (y_u^T R_y y_u + u^T R_u u) dt. \tag{14}$$

$C$). We derive Kalman filter parameters $K_c^{LQG}$ and $K_f^{LQG}$. They minimize $J_u$ and they are evaluated analytically using the solution $X^*$ and $Y^*$ of the following AREs:

$$\begin{aligned} &X A_u + A_u^T X - X B_u R_u^{-1} {B_u}^T X + {C_u}^T R_y C_u = 0, \quad X = X^T, \\ &Y A_u^T + A_u Y - Y {C_u}^T V^{-1} C_u Y + B_w W B_w^T = 0, \quad Y = Y^T, \end{aligned} \tag{15}$$

by $K_c^{LQG} = R_u^{-1} B_u^T X^*$ and $K_f^{LQG} = V^{-T} C_u Y^*$.

$D$). In the algorithm we consider $\vartheta_2 = (K_c^{LQG}, K_f^{LQG})$.

$E$). In this case, no dynamic filter is involved for the performance channel, so that $x_2$ is removed from (9).

$F$). In (9), $C_{22} = 0$ and the other involved matrices are specified as follows

$$B_2 = \begin{pmatrix} (B_w W B_w)^{1/2} & 0 \end{pmatrix}, \ C_2 = \begin{pmatrix} (C_u^T R_y C_u)^{1/2} \\ 0 \end{pmatrix}, \ D_{2u} = \begin{pmatrix} 0 \\ R_u^{1/2} \end{pmatrix}, \ D_{y2} = \begin{pmatrix} 0 & V^{1/2} \end{pmatrix}.$$

To specify the $H_\infty$ channel matrices in (9), we proceed as follows:

$\alpha$). We choose a low-pass weighting filter $F_{\infty 1}(s)$ at the control input to limit the maximum effort at low frequencies, i.e. $z_{\infty 1}(s) = F_{\infty 1}(s)u(s)$.

$\beta$). We choose a high-pass weighting filter $F_{\infty 2}(s)$ at the output to reduce the amplitude of oscillations, i.e. $z_{\infty 2}(s) = F_{\infty 2}(s)y(s)$.

$\gamma$). Denoting their associated state space representations by, $(A_{\infty_1}, B_{\infty_1}, C_{\infty_1}, D_{\infty_1} = 0)$ and $(A_{\infty_2}, B_{\infty_2}, C_{\infty_2}, D_{\infty_2})$, it can be easily verified that in (9)

$$A_{\infty\infty} = \begin{pmatrix} A_{\infty_1} & 0 \\ 0 & A_{\infty_2} \end{pmatrix}, \; A_{\infty} = \begin{pmatrix} 0 \\ B_{\infty_2} C_u \end{pmatrix}, \; B_{\infty u} = \begin{pmatrix} B_{\infty_1} \\ 0 \end{pmatrix},$$

$$C_{\infty} = \begin{pmatrix} 0 \\ D_{\infty_2} C_u \end{pmatrix}, \; C_{\infty\infty} = \begin{pmatrix} C_{\infty_1} & 0 \\ 0 & C_{\infty_2} \end{pmatrix}, \; D_{\infty u} = 0, \; D_{\infty\infty} = 0, \; D_{y\infty} = 0.$$

Note that the transfer operator $T_{z_\infty w_\infty}(\vartheta)$ includes the two transfer blocks $z_{\infty 1}/w_\infty$ and $z_{\infty 2}/w_\infty$ shown in Figure 1:

$$T_{z_\infty w_\infty} = \begin{bmatrix} z_{\infty 1}/w_\infty \\ z_{\infty 2}/w_\infty \end{bmatrix} = \begin{bmatrix} F_{\infty 1} S_i(\vartheta) \\ F_{\infty 2} P S_i(\vartheta) \end{bmatrix}, \tag{16}$$

where $S_i = (I+KP)^{-1}$ is the input sensitivity function. The filter $F_{\infty 1}$ is a high-pass, $F_{\infty 2}$ is a low-pass. This reflects the fact that in the channel $w_\infty \to z_{\infty 1}$ we want to penalize high frequency components of the control signal, while in $z_{\infty 2}$ we want the low frequency components of the output $y$ to track the reference input $r = 0$. For more details on how to choose filters in a robust control synthesis, see (Zhou and Doyle, 1998; Doyle et al. 1982)

**Remark 4.** The control scenario chosen in Figure 1 does not only robustify the design against the *external* effect of process noise $w_\infty$, but also against *intrinsic* uncertainty in controller and plant, as we now argue.

Indeed, by (16) the transfer function of the first robustness channel $w_\infty \to u \to z_{\infty 1}$ involves the input sensitivity function $S_i = (I + KP)^{-1}$. In Figure 1 we have $u = Ke$, $e = -y$, $y = Pu$ and if we consider the scheme without the inputs and differentiate with respect to $K$, keeping $P$ fixed, we obtain $du = K \cdot de + dK \cdot e$, $de = -dy$, $dy = Pdu$, hence

$$du = (I + KP)^{-1} (dK \cdot e) = S_i (dK \cdot e).$$

Since optimization tries to keep the operator norm $\|S_i\|_\infty = \|S_i\|_{2,2}$ small, it also minimizes the effect $du$ of a variation $dK$ in the controller variable. Therefore we can say the first robustness channel reduces undesirable high frequency effects caused by a variation $dK$ in the nominal controller variable.

Similarly, if we want to minimize effects caused by variations in the system $P$, we differentiate with respect to $P$, keeping $K$ fixed. That gives $du = K \cdot de$, $dy = P \cdot du + dP \cdot u$, $de = -dy$, hence

$$dy = (I + PK)^{-1} (dP \cdot u) =: S_o (dP \cdot u),$$

now involving the output sensitivity function $S_o = (I + PK)^{-1}$. So normally, in order to reduce high frequency effects of a variation $dP$ in the plant parameters on the output $y$, we ought to add yet another robustness constraint based on $S_o$. However, we consider here the case $m = p = 1$ where the channels are SISO and we have $KP = PK$, hence $S_i = S_o$, and in the present study $S_o$ is therefore not required.

In conclusion we can say that, as promised, the synthesis scheme in Figure 1 robustifies the design against undesirable effects caused by unstructured internal variations $dP$ in $P$. Since system reduction is heavily used and can be understood as such an effect, this justifies the choice of the robustness channels (16). For more details on how to choose filters in a robust control synthesis, see (Zhou and Doyle, 1998; Doyle et al. 1982). For other choices of sensitivity functions classified by the type of perturbation in the system see Doyle (Doyle et al. 1990).

## 6. Proof of the main result

In this section we prove Proposition 2 and Theorem 3 given in the section 4. We treat the channels separately, which is possible by construction. That means, we consider

$$S_u : \begin{cases} \dot{x}_u = A_u x_u \qquad\qquad + B_{fu}w + B_u u \\ \dot{x}_f^u = A_{fu}x_u + A_{ff}x_f^u + B_{ff}w + B_{fu}u \\ z_u = C_{fu}x_u + C_{ff}x_f^u + D_{ff}w + D_{fu}u \\ y_u = C_u x_u \qquad\qquad + D_{yf}w \end{cases} \qquad \mathcal{S} : \begin{cases} \dot{\mathbf{x}} = \mathcal{A}\mathbf{x} \qquad\qquad + \mathcal{B}_f w + \mathcal{B}u \\ \dot{x}_f = \mathcal{A}_f\mathbf{x} + A_{ff}x_f + B_{ff}w + B_{fu}u \\ z = \mathcal{C}_f\mathbf{x} + C_{ff}x_f + D_{ff}w + D_{fu}u \\ y = \mathcal{C}\mathbf{x} \qquad\qquad + D_{yf}w. \end{cases}$$

where $f$ stands for any of the filters $f = 2$ or $f = \infty$. Note that in the case $f = 2$ we must have $D_{22} = 0$. Recall that

$$\begin{aligned} &A_u = \mathcal{F}_u^T\mathcal{A}\mathcal{E}_u,\ A_{fu} = \mathcal{A}_f\mathcal{E}_u,\ B_u = \mathcal{F}_u^T\mathcal{B},\ B_{fu} = \mathcal{F}_u^T\mathcal{B}_f, \\ &C_{fu} = \mathcal{C}_f\mathcal{E}_u,\ C_u = \mathcal{C}\mathcal{E}_u. \end{aligned} \tag{17}$$

Note that on the left only the unstable subsystem $S_u$ is taken care of, as according to our procedure the stable system $\mathcal{S}_s$ remains uncontrolled. We consider the following observer-based controller for $S_u$ in the reduced space

$$u(s) = -K_c(sI - (A_u - B_uK_c - K_f^TC_u))^{-1}K_f^Ty_u(s),$$

parametrized by $\vartheta = (K_c, K_f)$, and the observer-based controller

$$u(s) = -\mathcal{K}_c(s\mathcal{I} - (\mathcal{A} - \mathcal{B}\mathcal{K}_c - \mathcal{K}_f^T\mathcal{C}))^{-1}\mathcal{K}_f^Ty(s)$$

for the large dimensional space $\mathcal{S}$, parametrized by $\theta = (\mathcal{K}_c, \mathcal{K}_f)$. Substituting them in $S_u$, respectively, $\mathcal{S}$, gives the closed loop systems $(S_u)^{cl}$, respectively, $\mathcal{S}^{cl}$:

$$(S_u)^{cl} : \begin{cases} \dot{x}_u = A_ux_u - B_uK_c\widehat{x}_u + B_{fu}w \\ \dot{\widehat{x}}_u = A_u\widehat{x}_u - B_uK_c\widehat{x}_u + K_f^T(y_u - \widehat{y}_u) \\ \dot{x}_f^u = A_{ff}x_f^u + A_{fu}x_u - B_{fu}K_c\widehat{x}_u + B_{ff}w \\ z_u = C_{fu}x_u + C_{ff}x_f^u - D_{fu}K_c\widehat{x}_u + D_{fw}w \\ y_u = C_ux_u + D_{yf}w, \\ \widehat{y}_u = C_u\widehat{x}_u \end{cases} \quad \mathcal{S}^{cl} : \begin{cases} \dot{\mathbf{x}} = \mathcal{A}\mathbf{x} - \mathcal{B}\mathcal{K}_c\widehat{\mathbf{x}} + \mathcal{B}_fw \\ \dot{\widehat{\mathbf{x}}} = \mathcal{A}\widehat{\mathbf{x}} - \mathcal{B}\mathcal{K}_c\widehat{\mathbf{x}} + \mathcal{K}_f^T(y - \widehat{y}) \\ \dot{x}_f = A_{ff}x_f + \mathcal{A}_f\mathbf{x} - B_{fu}\mathcal{K}_c\widehat{\mathbf{x}} + B_{ff}w \\ z = \mathcal{C}_f\mathbf{x} + C_{ff}x_f - D_{fu}\mathcal{K}_c\widehat{\mathbf{x}} + D_{fw}w \\ y = \mathcal{C}\mathbf{x} + D_{yf}w \\ \hat{y} = \mathcal{C}\widehat{\mathbf{x}} \end{cases}$$

Inspired by the PEVA algorithm, we decompose $\mathbf{x}$ and $\widehat{\mathbf{x}}$ as follows

$$\mathbf{x} = \mathcal{E}_ux_u + \mathcal{E}_s\mathbf{x}_s, \quad \widehat{\mathbf{x}} = \mathcal{E}_u\widehat{x}_u + \mathcal{E}_s\widehat{\mathbf{x}}_s,$$

and at the same time, we replace $\mathcal{K}_c$ and $\mathcal{K}_f$ by $K_c = \mathcal{K}_c\mathcal{F}_u^T$ and $K_f = \mathcal{K}_f\mathcal{E}_u^T$, i.e. $\theta = \theta(\vartheta)$. These actions result in

$$(S^{cl})_u : \begin{cases} \dot{x}_u = A_ux_u - B_uK_c\widehat{x}_u + B_{fu}w \\ \dot{\hat{x}}_u = A_u\hat{x}_u - B_uK_c\widehat{x}_u + K_f^T(y_u - \widehat{y}_u + y_s - \widehat{y}_s) \\ \dot{x}_f^u = A_{ff}x_f^u + A_{fu}x_u - B_{fu}K_c\widehat{x}_u + B_{ff}w \\ z_u = C_{fu}x_u + C_{ff}x_f^u - D_{fu}K_c\widehat{x}_u + D_{fw}w \\ y_u = C_ux_u + D_{yf}w \\ \widehat{y}_u = C_u\widehat{x}_u \end{cases} \quad (\mathcal{S}^{cl})_s : \begin{cases} \dot{\mathbf{x}}_s = \mathcal{A}_s\mathbf{x}_s - \mathcal{B}_sK_c\hat{x}_u + \mathcal{B}_{fs}w \\ \dot{\hat{\mathbf{x}}}_s = \mathcal{A}_s\hat{\mathbf{x}}_s - \mathcal{B}_sK_c\hat{x}_u \\ \dot{x}_f^s = A_{ff}x_f^s + \mathcal{A}_{fs}\mathbf{x}_s \\ z_s = \mathcal{C}_{fs}\mathbf{x}_s + C_{ff}x_f^s \\ y_s = \mathcal{C}_s\mathbf{x}_s \\ \hat{y}_s = \mathcal{C}_s\hat{\mathbf{x}}_s, \end{cases}$$

where

$$\mathcal{A}_{fs} = \mathcal{A}_f\mathcal{E}_s, \quad \mathcal{B}_s = \mathcal{F}_s^T\mathcal{B}, \quad \mathcal{B}_{fs} = \mathcal{F}_s^T\mathcal{B}_f, \quad \mathcal{C}_{fs} = \mathcal{C}_f\mathcal{E}_s.$$

Please recall that the notation $(S^{cl})_u$ is chosen only to emphasize the similarity between this subsystem and $(S_u)^{cl}$ and it does not mean that it is unstable!
We can present the following findings:

a. The closed-loop system $\mathcal{S}^{cl}$ can be fully recovered from the two split closed-loop systems $(S^{cl})_u$ and $(\mathcal{S}^{cl})_s$, as long as the controller $\mathcal{K}(\theta)$ is pulled back from some $K(\vartheta)$ via (13).
b. This is no longer the case if the closed-loop system $(S_u)^{cl}$ is used instead of $(S^{cl})_u$. In particular $(S_u)^{cl} \neq (S^{cl})_u$.
c. $(\mathcal{S}^{cl})_s$ and $(\mathcal{S}^{cl})$ feature big matrices, indicated by the boldface and calligraphic elements, but the $u$-operator applied to $\mathcal{S}^{cl}$ makes $(S^{cl})_u$ a small system.
d. The term which makes the difference between $(S^{cl})_u$ and $(S_u)^{cl}$ is

$$K_f^T(y_s - \widehat{y}_s) = K_f^T\mathcal{C}_s(\mathbf{x}_s - \widehat{\mathbf{x}}_s).$$

In particular, this term causes trouble, as the big matrix $\mathcal{C}_s$ and the state $\mathbf{x}_s$ are involved.

**Remark 5.** Concerning item a., the equations of $\mathcal{S}^{cl}$ are obtained by combining those of $(S^{cl})_u$ and $(\mathcal{S}^{cl})_s$ bearing in mind that $\mathbf{x} = \mathcal{E}_u x_u + \mathcal{E}_s\mathbf{x}_s = \mathcal{E}[x_u,\ \mathbf{x}_s]^T$, $\hat{\mathbf{x}} = \mathcal{E}_u\hat{x}_u + \mathcal{E}_s\hat{\mathbf{x}}_s = \mathcal{E}[\hat{x}_u,\ \hat{\mathbf{x}}_s]^T$, $y = y_u + y_s$, $x_f = x_f^u + x_f^s$ and $z = z_u + z_s$. Then we have to use the following properties to derive the equations:

$$\begin{aligned} &\mathcal{F}_u^T\mathcal{B}\mathcal{K}_c\widehat{\mathbf{x}} = B_uK_c\widehat{x}_u, \qquad && \mathcal{F}_u^T\mathcal{K}_f^T(y-\hat{y}) = K_f^T(y-\hat{y})\\ &\mathcal{F}_s^T\mathcal{B}\mathcal{K}_c\widehat{\mathbf{x}} = \mathcal{B}_sK_c\widehat{x}_u, \qquad && \mathcal{F}_s^T\mathcal{K}_f^T(y-\hat{y}) = 0. \end{aligned} \tag{18}$$

□

The question is now how we deal with the mismatch between $(S_u)^{cl}$ and $(S^{cl})_u$. The term $(y_u - \widehat{y}_u + y_s - \widehat{y}_s)$ in $(S^{cl})_u$ can be expanded as:

$$y_u - \widehat{y}_u + y_s - \widehat{y}_s = C_u(x_u - \hat{x}_u) + \mathcal{C}_se^{\mathcal{A}_st} * \mathcal{B}_{fs}w + D_{yf}w, \tag{19}$$

where $*$ is the convolution operator. This equation will be required later.

**6.1. *Proof of proposition 2.*** Consider the reduced system $(S_u)^{cl}$. We introduce a new state variable $e_u = x_u - \widehat{x}_u$, rewriting the state equations of $(S_u)^{cl}$ as:

$$\begin{pmatrix} \dot{x}_f^u \\ \dot{\hat{x}}_u \\ \dot{e}_u \end{pmatrix} = \begin{pmatrix} A_{ff} & A_{fu} - B_{fu}K_c & A_{fu} \\ 0 & A_u - B_uK_c & K_f^TC_u \\ 0 & 0 & A_u - K_f^TC_u \end{pmatrix} \begin{pmatrix} x_f^u \\ \hat{x}_u \\ e_u \end{pmatrix} + \begin{pmatrix} B_{ff}w \\ 0 \\ B_{fu}w \end{pmatrix}.$$

Since by hypothesis the controller $K(\vartheta)$ with $\vartheta = (K_c, K_f)$ is stabilizing, $(S_u)^{cl}$ is stable, which means $A_{ff}$, $A_u - B_uK_c$ and $A_u - K_f^TC_u$ are stable. This uses the fact that the filter $A_{ff}$ is stable by construction.

Let us get back with this information to the large scale closed-loop system $\mathcal{S}^{cl}$. Introducing two similar state variables $e_u = x_u - \widehat{x}_u$ and $\mathbf{e}_s = \mathbf{x}_s - \widehat{\mathbf{x}}_s$, using (19) we get the following equivalent state equations for $\mathcal{S}^{cl}$:

$$\begin{pmatrix} \dot{x}_f \\ \dot{\mathbf{x}}_s \\ \dot{\hat{x}}_u \\ \dot{e}_u \\ \dot{\mathbf{e}}_s \end{pmatrix} = \begin{pmatrix} A_{ff} & \mathcal{A}_{fs} & A_{fu} - B_{fu}K_c & A_{fu} & 0 \\ 0 & \mathcal{A}_s & -\mathcal{B}_sK_c & 0 & 0 \\ 0 & 0 & A_u - B_uK_c & K_f^TC_u & 0 \\ 0 & 0 & 0 & A_u - K_f^TC_u & 0 \\ 0 & 0 & 0 & 0 & \mathcal{A}_s \end{pmatrix} \begin{pmatrix} x_f \\ \mathbf{x}_s \\ \widehat{x}_u \\ e_u \\ \mathbf{e}_s \end{pmatrix}$$
$$+ \begin{pmatrix} B_{ff}w \\ \mathcal{B}_{fs}w \\ K_f^T\mathcal{C}_se^{\mathcal{A}_st} * \mathcal{B}_{fs}w + K_f^TD_{yf}w \\ B_{fu}w - K_f^T\mathcal{C}_se^{\mathcal{A}_st} * \mathcal{B}_{fs}w - K_f^TD_{yf}w \\ \mathcal{B}_{fs}w \end{pmatrix},$$

where $*$ is the convolution operator. Since $\mathcal{A}_s$ is stable by the PEVA construction, the stability of $A_{ff}$, $A_u - B_u K_c$ and $A_u - K_f^T C_u$ established above shows that the closed loop system $\mathcal{S}^{cl}$ remains stable. Note that we again use the fact that $\mathcal{K}(\theta)$ is pulled back from $K(\vartheta)$ via (13), so that the elements $\mathcal{K}_c$, $\mathcal{K}_f$ can be expressed with the help of $K_c$ and $K_f$. We recall again that this observer-based stabilizing controller is of the same order as the system. In tandem with (18) that completes the proof of Proposition 2. □

**6.2. *Links between the transfer functions* $T_{z_u w}(\vartheta)$ *and* $T_{zw}(\theta)$.** In the following we need new notations for the states in $(S_u)^{cl}$, as they must be distinguished from those in $(S^{cl})_u$. The subscript $u$ in $(S_u)^{cl}$ is hence replaced by $r$. We now establish a link between the transfer functions $T_{z_r w}(\vartheta)$ and $T_{zw}(\theta)$.

**Proposition 4.** *There exist transfer functions $H_i(s)$ $i = 1, \ldots, 6$, independent of $\vartheta$ and $\theta$, such that for every controller $K(\vartheta)$ in reduced space and its pull back $\mathcal{K}(\theta)$ in large space the following relations in closed-loop are satisfied:*

$$
\begin{aligned}
T_{z_r w}(s,\vartheta) &= H_1(s) \cdot H_r(s,\vartheta) + H_2(s), \\
H_r(s,\vartheta) &= H_t(s,\vartheta) \cdot H_3(s), \\
H(s,\vartheta) &= H_t(s,\vartheta) \cdot H_4(s) \\
T_{zw}(s,\theta) &= H_5(s) \cdot H(s,\vartheta) + H_6(s), \quad \theta = \theta(\vartheta).
\end{aligned} \tag{20}
$$

*Here $\vartheta = (K_c, K_f)$. The parameter dependent transfer functions $H_r(s,\vartheta)$ and $H(s,\vartheta)$ are given as $H(s,\vartheta) = -K_c \cdot \hat{x}_u(s,\vartheta)/w(s)$ and $H_r(s,\vartheta) = -K_c \cdot \hat{x}_r(s,\vartheta)/w(s)$, while $H_t(s,\vartheta)$ is given in formula* (21) *below.*

*Proof.* We start by observing that the transfer function of $(S^{cl})_s$ is obtained through

$$
\begin{aligned}
\mathbf{x}_s(s) &= (sI - \mathcal{A}_s)^{-1} \cdot \mathcal{B}_s \cdot (-K_c \widehat{x}_u(s)) + (sI - \mathcal{A}_s)^{-1} \cdot \mathcal{B}_{fs} \cdot w(s) \\
x_f^s(s) &= (sI - A_{ff})^{-1} \cdot \mathcal{A}_{fs} \cdot \mathbf{x}_s(s) = M_1(s) \cdot (-K_c \widehat{x}_u(s)) + M_2(s) w(s),
\end{aligned}
$$

where

$$
\begin{aligned}
M_1(s) &= (sI - A_{ff})^{-1} \cdot \mathcal{A}_{fs} \cdot (sI - \mathcal{A}_s)^{-1} \mathcal{B}_s, \\
M_2(s) &= (sI - A_{ff})^{-1} \cdot \mathcal{A}_{fs} \cdot (sI - \mathcal{A}_s)^{-1} \mathcal{B}_{fs}.
\end{aligned}
$$

The equations of $(S^{cl})_u$ provide

$$
\begin{aligned}
x_u(s) &= (sI - A_u)^{-1} \cdot B_u \cdot (-K_c \hat{x}_u(s)) + (sI - A_u)^{-1} \cdot B_{fu} w(s) \\
x_f^u(s) &= (sI - A_{ff})^{-1} A_{fu} x_u(s) + (sI - A_{ff})^{-1} B_{fu}(-K_c \widehat{x}_u(s)) + (sI - A_{ff})^{-1} B_{ff} w(s) \\
&= N_1(s) \cdot (-K_c \widehat{x}_u(s)) + N_2(s) w(s),
\end{aligned}
$$

where

$$
\begin{aligned}
N_1(s) &= (sI - A_{ff})^{-1} B_{fu} + (sI - A_{ff})^{-1} A_{fu} (sI - A_u)^{-1} B_u, \\
N_2(s) &= (sI - A_{ff})^{-1} B_{ff} + (sI - A_{ff})^{-1} A_{fu} (sI - A_u)^{-1} B_{fu}.
\end{aligned}
$$

Via the equations of $(S^{cl})_u$ we also define a very useful transfer function from $w$ to $-K_c \cdot \widehat{x}_u$

$$
H(s,\vartheta) := -K_c \cdot \widehat{x}_u(s)/w(s) = H_t(s,\vartheta) H_4(s),
$$

where

$$
H_t(s,\vartheta) = \frac{-K_c (sI - A)^{-1} K_f^T}{(I + (sI - A)^{-1} K f^T C_u N_1(s) K_c)} \tag{21}
$$

and

$$H_4(s) = C_u N_2(s) + \mathcal{C}_s(s\mathcal{I} - \mathcal{A}_s)^{-1}\mathcal{B}_{fs} + D_{yf}. \tag{22}$$

Using the transfer function $H(s,\vartheta)$, which for short is denoted by $H(.)$, and remembering the pull back operator $\vartheta \to \theta$, we can write:

$$\begin{aligned} z_u(s,\theta) &= [C_{fu}\cdot(sI - A_u)^{-1}B_u + C_{ff}\cdot N_1(s) + D_{fu}]\cdot H(.) \\ &\quad + [C_{fu}\cdot(sI - A_u)^{-1}B_{fu} + C_{ff}\cdot N_2(s) + D_{fu}]\cdot w(s), \\ z_s(s,\theta) &= [\mathcal{C}_{fs}\cdot(s\mathcal{I} - \mathcal{A}_s)^{-1}\cdot\mathcal{B}_s + C_{ff}\cdot M_1(s)]\cdot H(.) \\ &\quad + [\mathcal{C}_{fs}\cdot(s\mathcal{I} - \mathcal{A}_s)^{-1}\cdot\mathcal{B}_{fs} + C_{ff}\cdot M_2(s)]\cdot w(s). \end{aligned} \tag{23}$$

Recall that,

$$\begin{aligned} T_{zw}(s,\theta) &= z(s,\theta)/w(s) \\ T_{z_u w}(s,\theta) &= z_u(s,\theta)/w(s) \\ T_{z_s w}(s,\theta) &= z_s(s,\theta)/w(s), \end{aligned} \tag{24}$$

then, regarding $z(.) = z_u(.) + z_s(.)$ and the relations (23), (24), we find out

$$T_{zw}(s,\theta) = H_5(s)\cdot H(s,\vartheta) + H_6(s),$$

where

$$H_5(s) = C_{fu}\cdot(sI - A_u)^{-1}B_u + \mathcal{C}_{fs}\cdot(s\mathcal{I} - \mathcal{A}_s)^{-1}\cdot\mathcal{B}_s + C_{ff}(N_1(s) + M_1(s)) + D_{fu} \tag{25}$$

and

$$H_6(s) = C_{fu}\cdot(sI - A_u)^{-1}B_{fu} + \mathcal{C}_{fs}\cdot(s\mathcal{I} - \mathcal{A}_s)^{-1}\cdot\mathcal{B}_{fs} + C_{ff}(N_2(s) + M_2(s)) + D_{fw}. \tag{26}$$

In the same way it can be shown that

$$T_{z_r w}(s,\theta) = H_1(s)H_r(s,\vartheta) + H_2(s),$$

where

$$H_1(s) = C_{fu}\cdot(sI - A_u)^{-1}B_u + C_{ff}N_1(s) + D_{fu}, \tag{27}$$

$$H_2(s) = C_{fu}\cdot(sI - A_u)^{-1}B_{fu} + C_{ff}N_2(s) + D_{fw}, \tag{28}$$

$$H_r(s,\vartheta) = H_t(s,\vartheta)\cdot H_3(s),$$

where

$$H_3(s) = (sI - A)^{-1}[C_u N_2(s) + D_{yf}] \tag{29}$$

and $H_t(s,\vartheta)$ is given in (21).

□

*Proof of Theorem* 3. Using (20) we can now write $T_{z_r w}(s)$ as a function of $T_{zw}(s)$ as stated in (8), namely, $T_{z_r w} := F_1(s)T_{zw}F_2(s) + F_3(s)$, where

$$\begin{aligned} F_1(s) &= H_1(s)H_5(s)^{-1}, \quad F_2(s) = H_4(s)^{-1}H_3(s), \\ F_3(s) &= -H_1(s)H_5(s)^{-1}H_6(s)H_4(s)^{-1}H_3(s) + H_2(s). \end{aligned} \tag{30}$$

Therefore, minimizing $\|T_{z_r w}\|$ is the same as minimizing $\|F_1 T_{zw} F_2 + F_3\|$, and similarly for the robustness constraint. □

We can also apply Proposition 4 in the opposite direction. Suppose we start out with

$$\begin{array}{ll} \text{minimize} & \mathcal{P}(\theta) = \|T_{z_2 w_2}(\cdot,\theta)\|_2 \\ \text{subject to} & \mathcal{R}(\theta) = \|T_{z_\infty w_\infty}(\cdot,\theta)\|_\infty \le \rho \\ & \theta = (\mathcal{K}_c, \mathcal{K}_f) \text{ closed-loop stabilizing} \end{array} \tag{31}$$

where the performance and robustness channels $T_{z_2 w_2}$ and $T_{z_\infty w_\infty}$ have now been designed in the large dimensional system, with a rationale similar to that described by Figure 1. Then using Proposition 4 we can find stable transition filters $\mathcal{F}_i^{(j)}$ to formulate the following optimization program in reduced space:

$$
(32) \qquad \begin{array}{ll} \text{minimize} & \|\mathcal{F}_1^{(2)} T_{z_{2u} w_2}(\cdot,\vartheta)\mathcal{F}_2^{(2)} + \mathcal{F}_3^{(2)}\|_2 \\ \text{subject to} & \|\mathcal{F}_1^{(\infty)} T_{z_{\infty u} w_\infty}(\cdot,\vartheta)\mathcal{F}_2^{(\infty)} + \mathcal{F}_3^{(\infty)}\|_\infty \leq \rho \\ & \vartheta = (K_c, K_f) \text{ closed-loop stabilizing} \end{array}
$$

such that the following is true:

**Corollary 5.** *Given the performance and robustness channels $T_{z_2 w_2}$ and $T_{z_\infty w_\infty}$ in the full dimensional space, the stable transition filters $\mathcal{F}_j^{(i)}$ can be found such that $\vartheta^*$ is a local minimum of* (32) *if and only if its pull back $\theta^*$ is a local minimum of* (31)*.*

*Proof.* Adopting the notation of Proposition 4, i.e. $\mathcal{F}$ standing for $\mathcal{F}^{(2)}$ and $\mathcal{F}^{(\infty)}$, we put

$$
\mathcal{F}_1(s) = H_5(s)H_1(s)^{-1}, \;\; \mathcal{F}_2(s) = H_3(s)^{-1}H_4(s),
$$
$$
\mathcal{F}_3(s) = -H_5(s)H_1(s)^{-1}H_2(s)H_3(s)^{-1}H_4(s) + H_6(s),
$$

then the filters $\mathcal{F}_i$, $i = 1, 2, 3$ are stable by Proposition 2.

□

**Remark 6.** The reason why we had to base our numerical approach on the tandem (8), (12), and not on (31), (32), is that the computation of the filters $\mathcal{F}_j^{(i)}$ requires computation of a full basis of the stable eigenspace (see (25) and (26)), which is currently not practical. In contrast, designing the channels in the low-order space via (12) has still the desired effect and is algorithmically possible.

## 7. Numerical Experiment

We apply our trade-off technique to the problem of controlling a two-dimensional linearized Navier-Stokes equations in closed loop. Only boundary control and boundary observations are used. The example consists of the case of a flow around a circular cylinder shown in Figure 2. The flow is in the rectangle $\Omega = [-1.5,\, 2.2] \times [0,\, 0.4]$, the cylinder is centered at $(0.25,\, 0.2)$ and its diameter is 0.1.

Let $(\mathbf{z}, \mathbf{p})$ be the solution of the two-dimensional linearized Navier-Stokes equations around its stationary solution $(\mathbf{z}_s, \mathbf{p}_s)$. Then following Jovanović and Bamieh, 2001:

$$
(33) \qquad \begin{cases} \partial_t \mathbf{z} + (\mathbf{z}_s \,.\, \nabla)\mathbf{z} + (\mathbf{z} \,.\, \nabla)\mathbf{z}_s - \nu\Delta\mathbf{z} + \nabla\mathbf{p} = 0, & \text{in} \quad \Omega \times (0,\infty) \\ \nabla \,.\, \mathbf{z} = 0 \quad \text{in} \quad \Omega, \quad \mathbf{z}(0) = \mathbf{z}_0 \quad \text{in} \quad \Omega & \\ \mathbf{z} = U_e \quad \text{on} \quad \Gamma_e \times (0,T) \quad \mathbf{z} = 0 \quad \text{on} \quad \Gamma_D \times (0,\infty) & \\ \mathbf{z} = \mathbf{z}_c \quad \text{on} \quad \Gamma_c \times (0,\infty), & \\ \sigma(\mathbf{z},\mathbf{p})n = 0 \quad \text{on} \quad \Gamma_N \times (0,\infty), & \end{cases}
$$

where $\mathbf{z} = \begin{pmatrix} z_1 \\ z_2 \end{pmatrix}$ represents the velocity field in $x_1$ (or $x$ or horizontal) and in $x_2$ (or $y$ or vertical) directions, $\mathbf{p}$ is the pressure, and $\sigma(\mathbf{z}, \mathbf{p})$ is the stress defined by

$$
\sigma(\mathbf{z},\mathbf{p}) = \frac{2}{\mathrm{Re}}\Phi(\mathbf{z}) - \mathbf{pI}, \quad \mathbf{\Phi}(\mathbf{z}) = \frac{\mathbf{1}}{\mathbf{2}}[(\nabla\mathbf{z}) + (\nabla\mathbf{z})^{\mathbf{T}}], \quad (\nabla\mathbf{z})_{\mathbf{ij}} = \frac{\partial \mathbf{z_i}}{\partial \mathbf{x_j}}.
$$

The Reynolds number is $\mathrm{Re} = \rho d_c U_m/\mu$, where $\rho > 0$, $\mu > 0$ are respectively the constant density and viscosity of the fluid, $d_c$ is the diameter of the cylinder, and $U_m$ a characteristic

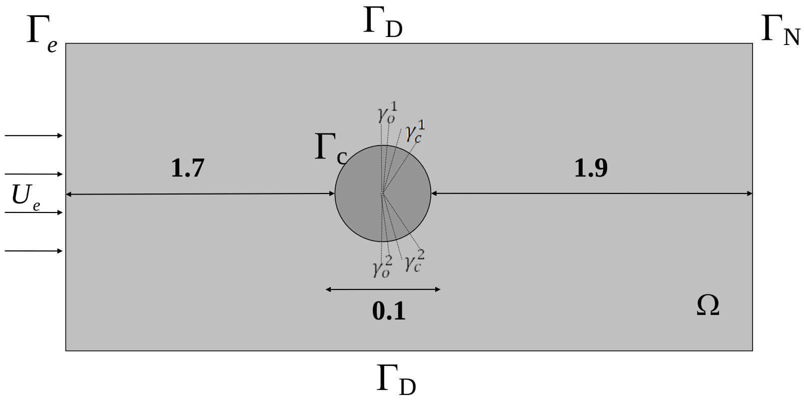


FIGURE 2. Sketch of the geometry for flow around a circular cylinder.

velocity associated with $\mathbf{z}_s$. As usual $\nu = \frac{\mu}{\rho}$ is kinematic viscosity and $\mathbf{I}$ is the identity tensor. It is assumed that $\rho = 1$, $U_m = 1$ and $d_c = 0.1$, which gives $\mathrm{Re} = \frac{0.1}{\mu}$.

We denote by $\Gamma$ the boundary of $\Omega$, and $\Gamma = \Gamma_e \cup \Gamma_N \cup \Gamma_D \cup \Gamma_c$. Control region $\Gamma_C \subset \Gamma_c$ is composed of two arcs $\gamma_c^1$ and $\gamma_c^2$ located at the perimeter of the disk between 70 and 80 degrees and $-70$ and $-80$ degrees, as shown in the Figure 2.
The boundary condition $\mathbf{z}_c$ is defined by

$$\mathbf{z}(t, \mathbf{x}(f)) = \begin{cases} u(t)m(f)n(\mathbf{x}(f)) & \text{at} \quad \gamma_c^1 \\ -u(t)m(f)n(\mathbf{x}(f)) & \text{at} \quad \gamma_c^2 \\ 0 & \text{at} \quad \Gamma_c \setminus \gamma_c^1 \cup \gamma_c^2 \end{cases},$$

where $\mathbf{x}(f)$ with $f \in [0, 1]$ parametrizes the boundaries $\gamma_c^i$, $i = 1, 2$. $n(\mathbf{x}(f))$ represents the orthogonal unitary vector at $\Gamma_c$ while $m$ is a function which models a regular rectangle. The function $m$ describing the control action is given as

$$m(f) = g(10f - 1) - g(10f - 9),$$

where

$$g(a) = \begin{cases} 0 & a \leq -1 \\ 0.5 + a(0.9375 - a^2(0.625 - 0.1875\, a^2)) & -1 < a < 1 \\ 1 & a \geq 1 \end{cases}.$$

The measured output consists of the integral of vorticity on $\Gamma_O \subset \Gamma_c$, i.e.

$$\mathbf{y}(t) = \int_{\Gamma_O} \left( \frac{\partial z_2(t)}{\partial x_1} - \frac{\partial z_1(t)}{\partial x_2} \right) d\Gamma,$$

where $\Gamma_O = \gamma_o^1 \cup \gamma_o^2$ and $\gamma_o^i,\ i = 1, 2$ are situated at the top and the bottom of the cylinder between 89 and 91 degrees and -89 and -91 degrees (see Figure 2).

The goal of the study is to reduce the output oscillations, caused by the perturbation on the boundary control ($U_e = 0.2 + w_\infty$), with a minimum effort in the control input. Figure 3 shows two Bell type perturbations $w_\infty(t)$ considered here in simulations. Two

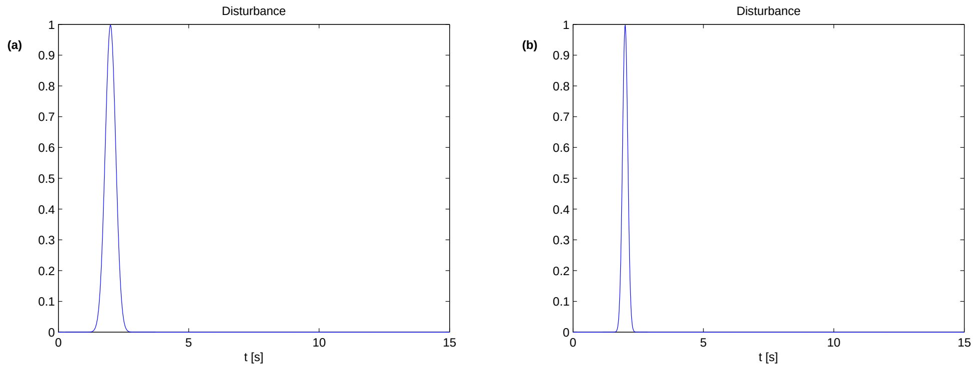


FIGURE 3. Bell type disturbances.

cases Re $= 80$ and Re $= 120$ have been studied. This needs linearization of the equations and other preliminaries, which are explained in the next subsection.

**7.1. *Preliminary operations.*** The physical system equations are discretized using a triangular mesh of 5791 nodes, symmetric with respect to the horizontal axis of the cylinder. A mixed Taylor-Hood finite element method of type P3-P2 was implemented in the COMSOL software (Comsol, 2012), which is used to find the descriptor system:

$$\begin{aligned} \mathcal{M}_{11}\dot{\mathfrak{z}}(t) &= \mathcal{A}_{11}\,\mathfrak{z}(t) + \mathcal{A}_{12}\mathfrak{p}(t) + \mathcal{B}_{u_1}\,u(t) + \mathcal{B}_{\infty 1}\,w_\infty(t) \\ 0 &= \mathcal{A}_{12}^T\,\mathfrak{z}(t) + \mathcal{B}_{u_2}\,u(t) \\ y(t) &= \mathcal{C}_1\,\mathfrak{z}(t) \end{aligned} \tag{34}$$

where $\mathfrak{z} \in \mathbb{R}^{n_z}$, $n_z = 33326$ and $\mathfrak{p} \in \mathbb{R}^{n_p}$, $n_p = 8136$ are respectively the states representing the velocity field and the ensemble of pressure and Lagrange multipliers. The mass matrix $\mathcal{M}_{11} \in \mathbb{R}^{n_z \times n_z}$ is symmetric positive definite. Control $u$ and output $y$ are both scalar, $w_\infty \in \mathcal{L}_2$ represents a bounded-energy disturbance at the boundary control $U_e$, sometimes referred to as process noise.

Following standard lines in fluid control, the next step consists in separating the $\mathfrak{z}$- and $\mathfrak{p}$-variables. This uses the Leray projector and we follow the method proposed in (Barbagallo et al. 2009), which introduces a new extended state $[\mathsf{z},\ \mathsf{p}]^T$ and a new control input $\mathsf{u} = \dot{u}$. This leads to a descriptor system of the form

$$\begin{aligned} \begin{pmatrix} \mathsf{M}_{11} & 0 \\ 0 & 0 \end{pmatrix} \frac{d}{dt}\begin{pmatrix} \mathsf{z} \\ \mathfrak{p} \end{pmatrix} &= \begin{pmatrix} \mathsf{A}_{11} & \mathsf{A}_{12} \\ \mathsf{A}_{12}^T & 0 \end{pmatrix}\begin{pmatrix} \mathsf{z} \\ \mathfrak{p} \end{pmatrix} + \begin{pmatrix} \mathsf{B}_1 \\ 0 \end{pmatrix}\mathsf{u} + \begin{pmatrix} \mathsf{B}_\infty \\ 0 \end{pmatrix} w_\infty \\ \mathsf{y} &= \mathsf{C}_1\mathsf{z}. \end{aligned} \tag{35}$$

For details we refer to the Appendix. At this stage we now employ the Leray projector

$$\pi = I - \mathsf{A}_{12}(\mathsf{A}_{12}^T\mathsf{M}_{11}^{-1}\mathsf{A}_{12})^{-1}\mathsf{A}_{12}^T\mathsf{M}_{11}^{-1},$$

to separate the $\mathsf{z}$- and $\mathfrak{p}$-variables. The interested reader is referred to (Heinkenschloss et al. 2008) for more details. As a result we obtain a system of the form

$$\begin{aligned} \dot{\mathbf{x}} &= \mathcal{A}\mathbf{x} + \mathcal{B}u + \mathcal{B}_\infty w_\infty \\ y &= \mathcal{C}\mathbf{x}. \end{aligned} \tag{36}$$

where $\mathbf{x} = \phi_l^T\mathsf{z}$ is in $\mathbb{R}^{(n_z-n_p)+1}$, $\pi = \phi_l\phi_r^T$, $\phi_l^T\phi_r = I$ and

$$\mathcal{A} = (\phi_r^T\mathsf{M}_{11}\phi_r)^{-1}\phi_r^T\mathsf{A}_{11}\phi_r,\ \ \mathcal{B} = (\phi_r^T\mathsf{M}_{11}\phi_r)^{-1}\phi_r^T\mathsf{B}_1,\ \ \mathcal{B}_\infty = (\phi_r^T\mathsf{M}_{11}\phi_r)^{-1}\phi_r^T\mathsf{B}_\infty,\ \ \mathcal{C} = \mathsf{C}_1\phi_r.$$

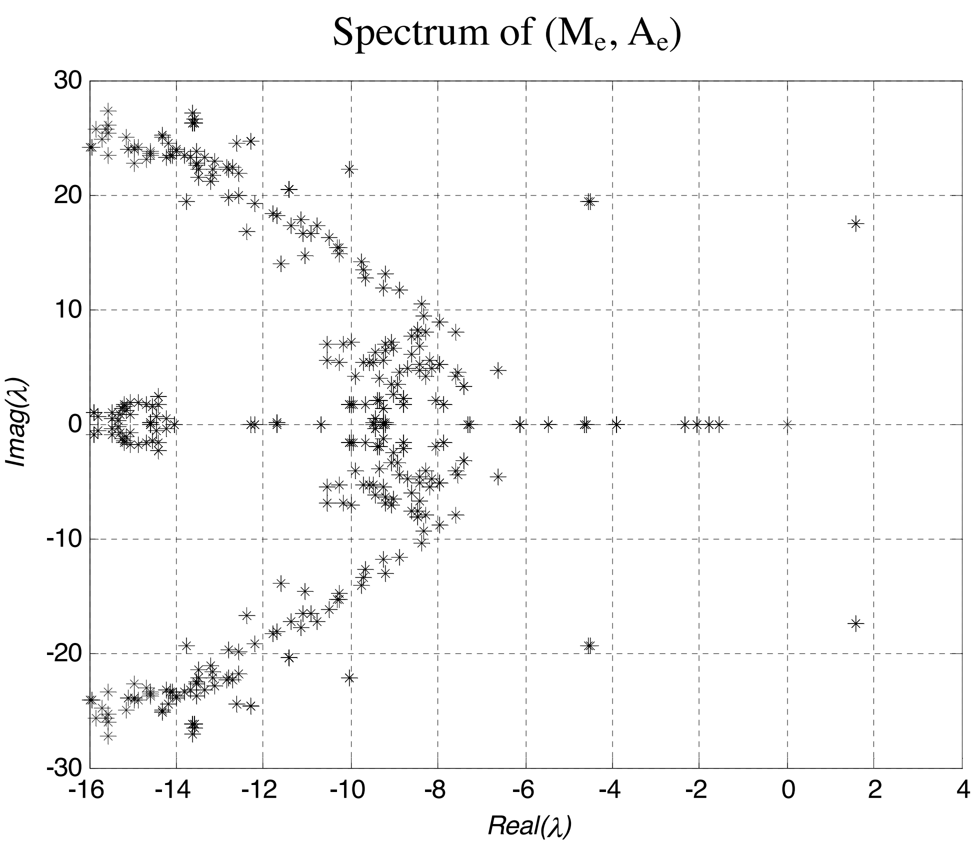


FIGURE 4. A part of the spectrum of $(\mathsf{M}, \mathsf{A})$ near the imaginary axis

This is the system $(\mathcal{S})$ which was the starting point of our theoretical development in section 2. To prepare the system above for the main algorithm, it is completed as

$$\begin{aligned} \dot{\mathbf{x}} &= \mathcal{A}\mathbf{x} + \mathcal{B}u + \mathcal{B}_2 w_2 + \mathcal{B}_\infty w_\infty \\ y &= \mathcal{C}\mathbf{x}. \end{aligned} \tag{37}$$

where $\mathcal{B}_2 = \mathcal{B}$ is chosen. This is a dynamical system in the $n_z - n_p + 1 = 25191$ dimensional subspace $\mathrm{null}(\pi)$.

**7.2. *Mixed synthesis.*** We explain next how the six steps of the algorithm are implemented.

**1) Initialization:**
In (Raymond and Thevenet, 2010; Thevenet, 2009), it is explained that the finite eigenvalues of $\mathcal{A}$ are the same as the finite generalized eigenvalues of $(\mathsf{M}, \mathsf{A})$, where

$$\mathsf{M} = \begin{pmatrix} \mathsf{M}_{11} & 0 \\ 0 & 0 \end{pmatrix}, \quad \mathsf{A} = \begin{pmatrix} \mathsf{A}_{11} & \mathsf{A}_{12} \\ \mathsf{A}_{12}^T & 0 \end{pmatrix}.$$

In addition, if we denote by $\mathsf{F}$ and $\mathsf{E}$ the right and the left generalized eigenvectors of $(\mathsf{M}, \mathsf{A})$ then $\mathcal{F} = \mathsf{MF}$, $\mathcal{E} = \mathsf{ME}$, which shows that in sections 4,5 and 6, we may replace $\mathcal{F}_u$, $\mathcal{F}_s$, $\mathcal{E}_u$, $\mathcal{E}_s$ by the corresponding matrices $\mathsf{MF}_u$, $\mathsf{MF}_s$, $\mathsf{ME}_u$, $\mathsf{ME}_s$.

Barkley (2006), considering a very similar setup, shows that for Reynolds numbers $50 \leq \mathrm{Re} \leq 255$ the spectrum of the linear operator features a conjugate pair of unstable eigenvalues. We use an Arnoldi method combined with a *shift and inverse* transformation implemented in the ARPACK library (Lehoucq et al., 1998) to compute the leading eigenvalues. For Re $=80$ and Re $=120$ the unstable modes are

$$\lambda_{\mathrm{Re}=80} = 1.5656 \mp 17.4217j \quad \lambda_{\mathrm{Re}=120} = 3.44 \mp 17.6j.$$

In the case Re $=80$ a part of the spectrum of $(\mathsf{M}, \mathsf{A})$ is shown in Figure 4. This system has three unstable poles at $1.56 \pm 17.3\,j$ and at 0. The pole at zero is introduced during transformation of the system (34) to the system (35), for more information see Appendix. The reduced-order system is hence at least of order 3, and can be larger if we decide to include some of the stable open-loop poles in $(S_u)$. In our experiment $n_u = 3$ is chosen. In the case Re $=120$ the reduced-order system is chosen of order 3.

**2) Define channels:**

Our goal is to compute a robustified version of the LQG controller according to section 5. To minimize the energy of the unstable states in the output, and also the energy of the control input, we choose $R_y = 1$ and $R_u = 1e-5$ in the performance index (14). The noise covariance matrices are $V = W = 1$.

In the case Re $=80$, filters specifying the $H_\infty$ channel are chosen by trial and error as

$$F_{\infty 1}(s) = \frac{10^4}{s + 2\,\pi\,5} \text{ and } F_{\infty 2}(s) = 10^{-4}\,\frac{s}{s + 2\,\pi\,5}.$$

In the case Re $=120$ we choose

$$F_{\infty 1}(s) = 10^7\,\frac{1}{s + 2\,\pi\,5} \text{ and } F_{\infty 2}(s) = 10^{-7}\,\frac{s}{s + 2\,\pi\,5}.$$

**3) Calibrate performance:**

The LQG controller $\vartheta_{LQG}$ is computed via AREs, given in (15). This controller is used as initial guess $\vartheta_2$ to calibrate robustness in step 4 of the algorithm.

**4) Calibrate robustness:**

The $\mathcal{H}_\infty$ program in step 4 is solved, leading to the solution $\vartheta_\infty$, which in turn is used to initialize the optimization program in step 5 of the algorithm.

**5) Mixed synthesis:**

In the mixed $\mathcal{H}_2/\mathcal{H}_\infty$-program in step 5, $r = \|T_{z_{\infty u} w}(\vartheta_\infty)\|_\infty + 10^{-5}$ is considered. This choice results in a mixed controller, which is as robust as the most robust controller $H_\infty$, but is expected to offer the desired compromise between performance and robustness.

**6) Evaluate performance:**

Due to the choice of $r$ very near its minimum $r_\downarrow$, the evaluation in step 6 of the algorithm shows that best robustness is achieved.

All the optimization programs were realized in Matlab using *Fmincon* from the optimization toolbox. Gradients and sub-gradients are computed analytically. The optimization programs use the nonsmooth algorithm, which is made available to users via the function *systune* in Robust Control Toolbox in MatlabR2013b. Simulation of the descriptor system is realized via the three stage second order backward difference formula.

The algorithm proposed for the trade-off behaves as expected, see table 1. Namely, in the case of the Reynolds number Re $=80$, and with the disturbance shown in Figure 3 (a), we obtain the nominal performance $\|T_{z_{2r} w_2}(\vartheta_2)\|_2^2 = 0.2394$, and the chosen robustness criterion gives $\|T_{z_{\infty r} w_\infty}(\vartheta_2)\|_\infty = 0.0663$. As this value is considered too

| Re | controller | $\|\cdot\|_2^2$ | $\|\cdot\|_\infty$ |
|---|---|---|---|
| 80 | LQG | 0.2394 | 0.0663 |
| | $\vartheta_\infty$ | 0.9066 | 0.0296 |
| | $\vartheta_{2/\infty}$ | 0.270 | 0.0296 |
| 120 | LQG | 1.3126 | 57.7968 |
| | $\vartheta_\infty$ | 5.98 | 24.26 |
| | $\vartheta_{2/\infty}$ | 1.5133 | 24.26 |

TABLE 1. Norms evaluated for different controllers and different Reynolds numbers.

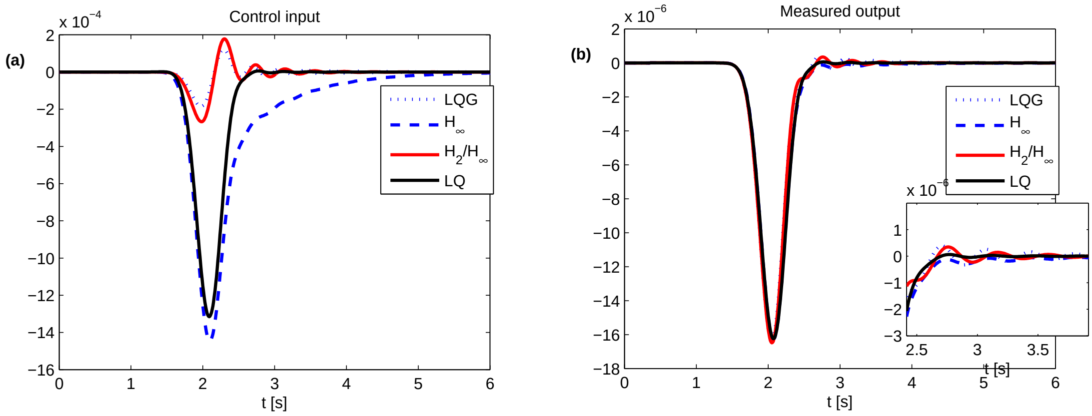


FIGURE 5. Results obtained for projected system $(\mathcal{S}_u)^{cl}$, when Re=80 and disturbance of Figure 3 (a).

large, we start the robustification procedure of Algorithm 1. The $H_\infty$-controller computed for the purpose of calibration has $\|T_{z_\infty r w_\infty}(\vartheta_\infty)\|_\infty = 0.0296$, which is the best robustness we can achieve. Naturally, this controller is made for robustness and not for performance, which is confirmed by the value $\|T_{z_{2r},w_2}(\vartheta_\infty)\|_2^2 = 0.9066$. The optimization procedure delivers the trade-off in the form of the mixed $H_2/H_\infty$-controller $\vartheta_{2/\infty}$. This controller achieves $\|T_{z_\infty r w_\infty}(\vartheta_{2/\infty})\|_\infty = 0.0296$, that is, the same robustness as $\vartheta_\infty$, but has $\|T_{z_{2r} w_2}(\vartheta_{2/\infty})\|_2^2 = 0.270$, which means a loss of performance of 12%. Performance of $\vartheta_{2/\infty}$ over $\vartheta_\infty$ is improved by 70.2%, while its robustness is preserved.

The advantage of the trade-off can also be shown via the control input and the measurement output time responses. Figures 5 (a) and (b) illustrate these signals in the case of the reduced-order system. We compare, respectively, control inputs and measured outputs obtained by different controllers. We also represent the responses obtained by the LQ regulator. The parameters of the LQ controller, i.e. the state feedback gains, are computed for the reduced-order system and are then pulled back to give the LQ parameters for full-order system: $\mathcal{K}_{LQ} = K_{LQ}\mathsf{F}_u^T\mathsf{M}$. Note that LQ is only a fictive controller, as it depends on knowledge of the full state $\mathbf{x}$, an unrealistic assumption in practice. However the LQ controller has the best possible robustness, and it can therefore be used to judge the quality of any candidate robust output feedback controller by inspecting whether its output resembles that of the LQ controller.

As can be seen, the observer-based $H_\infty$ controller indeed eliminates oscillations in the output faster than other observer-based controllers. However the price is a large control input effort. In contrast, the LQG controller economizes in its control input effort, but it is unacceptable as it authorizes larger oscillations. The mixed controller seems to give the best compromise, as indicated by its responses, which are situated between those of

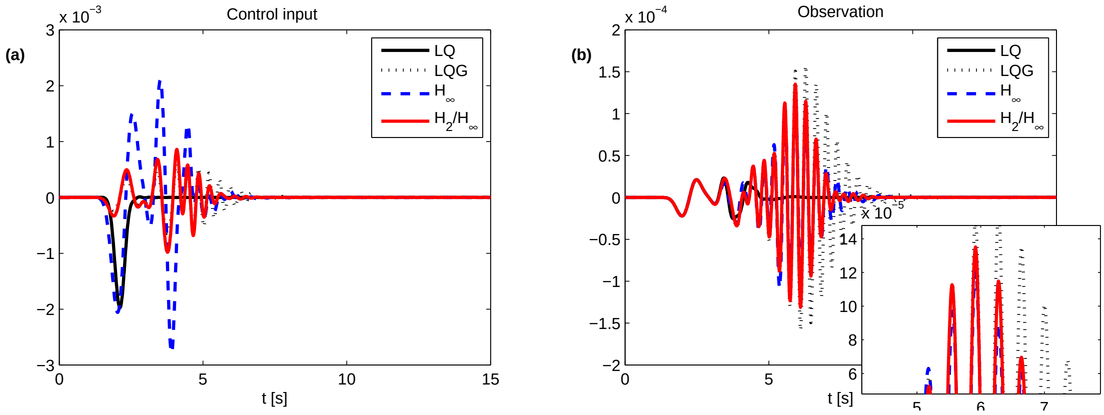


FIGURE 6. Results obtained for descriptor system $\mathcal{S}^{cl}$, when Re=80 and disturbance of Figure 3 (a).

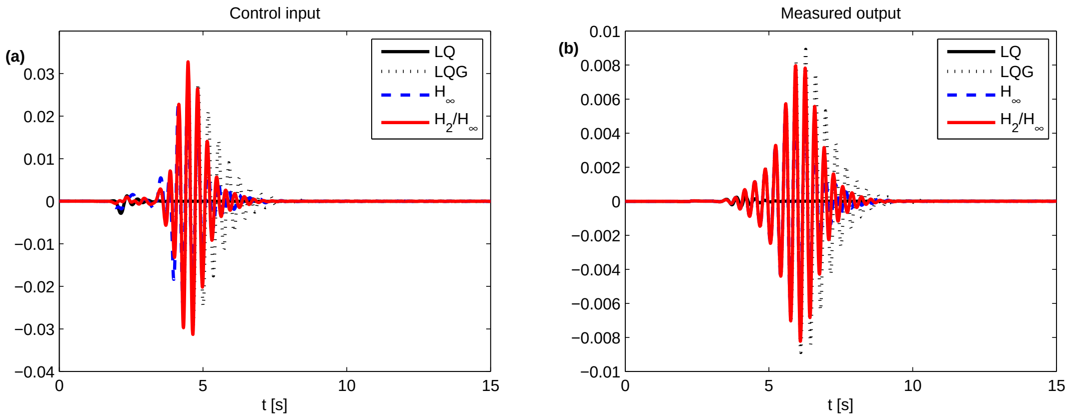


FIGURE 7. Results obtained for descriptor system when Re=80 and disturbance of Figure 3 (b).

the LQG and those of the $H_\infty$ controller. The mixed controller eliminates the oscillations faster than the LQG controller, and with much less control effort than the $H_\infty$ controller.

Figures 6 (a) and (b) compare the corresponding signals in the case of full-order system (descriptor system given in (35) of order 41462), i.e., when the controllers are pulled back to the full dimension. As can be seen, the output associated with the pulled back $H_\infty$ controller is in excellent agreement with the output of pulled back LQ controller. This confirms that the pulled back $H_\infty$ controller is the most robust observer-based controller. Once again, as in the reduced-order system case, oscillations in the measured output terminate more rapidly compared to the pulled back LQG controller while the control input effort is less than that of the pulled back $H_\infty$ controller. This means the trade-off organized in the reduced system is still present in the large state dimension, as we expected.

Figures 7 and 8 illustrate only the descriptor system results. Figure 7 compares the signals when a more active disturbance, shown in Figure 3 (b), is applied. Figure 8 concerns the descriptor system with larger Reynolds number, i.e. Re $=$ 120 and the perturbation of Figure 3 (a). As can be seen, the trade-off again carries over from the reduced system to the full system.

**Remark 7.** We recall that our controller is observer-based, hence its order is the same as the order of the linearized system. This system order may be very large and then simulation may be slow. For example simulation of a flow lasting 10 seconds for a system

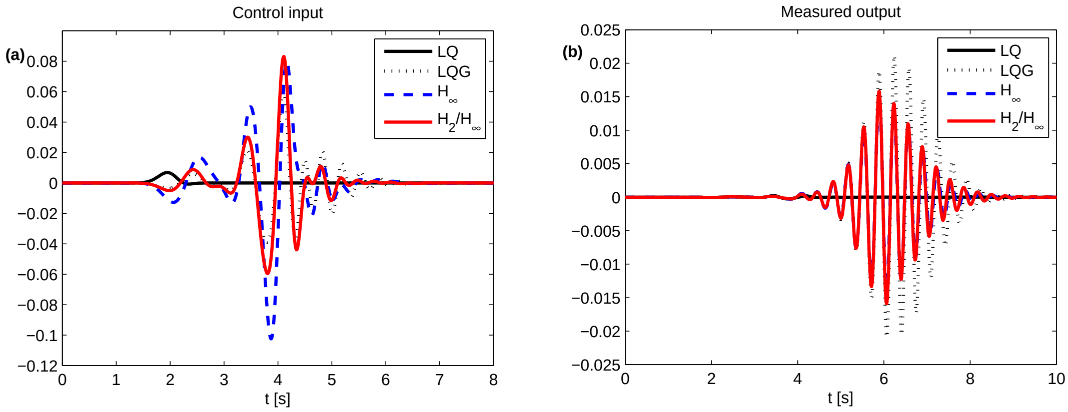


FIGURE 8. Results obtained for descriptor system when Re=120 and disturbance of Figure 3 (a).

with 300,000 states takes approximately 5 hours CPU even with a relatively large step of 0.001 s. For convenience, in the paper we have rather worked with 41,000 states, where the same simulation takes $\approx$ 8 seconds CPU. The large CPU in simulation is what we call the problem of *implementation*, and in the paper we do not pretend to propose a solution for this. What we propose is a solution to the problem of *computing* the controller i.e. the vectors $\mathcal{K}_c$ and $\mathcal{K}_f$. Namely, if the controller is to be robust with respect to system uncertainty, then it must be found by optimization, as we indicate. And then the size of $\mathcal{K}_c$, $\mathcal{K}_f$ becomes a serious problem, as the number $n$ of optimization variables is $n = \text{card}(\mathcal{K}_f) + \text{card}(\mathcal{K}_c)$. Since a non-linear optimization method has to be used, vectors $\mathcal{K}_c, \mathcal{K}_f \in \mathbb{R}^{500}$ are already highly challenging, and with currently known techniques it is out of the question to compute with $\mathcal{K}_c, \mathcal{K}_f \in \mathbb{R}^{41{,}000}$, let alone $\mathcal{K}_c, \mathcal{K}_f \in \mathbb{R}^{300{,}000}$. Therefore, for this large-scale system, a reduction technique like the one we propose has to be used.

## 8. Conclusion

We have presented a new method to realize a trade-off between performance and robustness in a class of large order linear systems via observer-based $H_2/H_\infty$ synthesis. The method does not require solving large scale Algebraic Riccati Equations, and instead uses nonlinear optimization problems of moderate size. The method is suited for systems with diagonalizable state space matrix and with a limited number of unstable modes.

By applying the PEVA algorithm to a large-order system in open loop, we obtain a reduced-order system whose order equals approximately the number of unstable modes in the large-order system.

We demonstrate that the stability of this reduced-order system in closed-loop leads to stability of the large system in closed-loop if a suitable *pull back procedure* for the controller is used. We then proceed to indicate that if a mixed $H_2/H_\infty$ performance and robustness trade-off is put to work in reduced space, then the results are approximately preserved when pulled back to the large dimension. We further demonstrate that the procedure leads to a significant reduction in the control effort, i.e., to a better performance, while maintaining the same level of robustness.

In its present form our approach is applicable in large scale pre-computations under the proviso that unstable eigenvalues and their associated eigenvectors are available, and as long as the order of the low-order system does not exceed ($\approx$ 500). For larger reduced systems the nonsmooth optimization algorithms are currently not very efficient. In some cases computation of the eigen decomposition may be the main bottleneck to our approach. For non-diagonalizable $\mathcal{A}$, or for large condition numbers, the approach of Varga (1995, 1981) may present an alternative.

In conclusion, we have presented a novel algorithmic solution to the problem of synthesizing an observer-based $H_2/H_\infty$ controller for a large-order system, by computing a suitable reduced-order system for which we cast an optimization problem representing a trade-off between performance and robustness, and by pulling the solution back to the large dimensional space.

The efficiency of our method was demonstrated in an application in fluid control where output oscillations caused by flow around a cylindrical obstacle had to be stabilized with constraints on the control effort. In simulations our novel controller attenuated oscillations caused by perturbation much faster than the optimal $H_2$ controller (LQG) and with lower control effort than the $H_\infty$ controller.

## Acknowledgment

This work was supported by FNRAE-project ECOSEA and by the Fondation EADS project Technicom.

## Appendix

The objective of this appendix is to explain how (35) is derived from (34). To simplify the notations, we re-write (34) as

$$\begin{aligned} M\dot{x}(t) &= A\,x(t) + B_1\,u(t) + B_2\,w_\infty(t) \\ y(t) &= C\,x(t) \end{aligned} \tag{38}$$

where $x = \begin{pmatrix} \mathfrak{z} \\ \mathfrak{p} \end{pmatrix}$ and

(39)

$$M = \begin{pmatrix} \mathcal{M}_{11} & 0 \\ 0 & 0 \end{pmatrix}, \quad A = \begin{pmatrix} \mathcal{A}_{11} & \mathcal{A}_{12} \\ \mathcal{A}_{12}^T & 0 \end{pmatrix}, \quad B_1 = \begin{pmatrix} \mathcal{B}_{u_1} \\ \mathcal{B}_{u_2} \end{pmatrix}, \quad B_2 = \begin{pmatrix} \mathcal{B}_{\infty 1} \\ 0 \end{pmatrix}, \quad C = \begin{pmatrix} \mathcal{C}_1 & 0 \end{pmatrix}.$$

We let $u(t) = \zeta(t)u_G$, where $u_G$ is the velocity profile of the injected or extracted flow, while $\zeta(t)$ determines its magnitude and temporal behavior. We take as the state vector $x$ the sum of the solution $x_h$ of the homogeneous problem, i.e. with no control input applied ($\zeta(t) = 0$), and a solution of the form $\zeta(t)x_s$, where $x_s$ is the stationary solution or the solution of the steady but inhomogeneous problem, i.e. when $\zeta(t) = u_0$, $w_\infty = 0$. Moreover, without loss of generality, we suppose that $u_0 = 1$. Then we have

- The homogeneous problem: $M\dot{x}_h = A\,x_h + B_2 w_\infty$.
- The inhomogeneous problem: $0 = A\,x_s + B_1$.

We express the state vector as $x = \zeta x_s + x_h$ and the control as $u = \zeta$ and substitute both in (38). This leads to:

$$\begin{aligned} M\dot{x}_h(t) &= A\,x_h(t) + (MA^{-1}B_1)\dot{\zeta}(t) + B_2\,w_\infty(t) \\ y(t) &= C\,x_h(t) + (-CA^{-1}B_1)\zeta(t). \end{aligned} \tag{40}$$

We define $B_h = MA^{-1}B_1$ and $C_h = \begin{pmatrix} C & -CA^{-1}B_1 \end{pmatrix}$. Due to the special form of $M$ we have $B_h = \begin{pmatrix} B_{h1} \\ 0_{n_p} \end{pmatrix}$.

If we replace in (40), $x_h$ by $\begin{pmatrix}\mathfrak{z}_h\\ \mathfrak{p}_h\end{pmatrix}$ and $M,\ A, ...$ by their equivalents from (39), we obtain

$$\begin{aligned}\mathcal{M}_{11}\dot{\mathfrak{z}}_h &= \mathcal{A}_{11}\mathfrak{z}_h + \mathcal{A}_{12}\mathfrak{p}_h + B_{h_1}\dot{\zeta} + \mathcal{B}_{\infty 1}w_\infty\\ 0 &= \mathcal{A}_{12}^T\mathfrak{z}_h\\ y &= \mathcal{C}_1\mathfrak{z}_h + (-CA^{-1}B_1)\zeta(t).\end{aligned}$$

In this last system, we consider $\zeta(t)$ as a new state variable, which results in the following extended system, which is the same as (35):

$$\begin{pmatrix}\mathsf{M}_{11} & 0\\ 0 & 0\end{pmatrix}\frac{d}{dt}\begin{pmatrix}\mathsf{z}\\ \mathsf{p}\end{pmatrix} = \begin{pmatrix}\mathsf{A}_{11} & \mathsf{A}_{12}\\ \mathsf{A}_{12}^T & 0\end{pmatrix}\begin{pmatrix}\mathsf{z}\\ \mathsf{p}\end{pmatrix} + \begin{pmatrix}\mathsf{B}_1\\ 0\end{pmatrix}\mathsf{u} + \begin{pmatrix}\mathsf{B}_\infty\\ 0\end{pmatrix}w_\infty$$
$$\mathsf{y} = \mathsf{C}_1\mathsf{z}.$$

Here we have $\mathsf{z} = \begin{pmatrix}\mathfrak{z}_h\\ \zeta\end{pmatrix}$, $\mathsf{p} = \mathfrak{p}_h$, $\mathsf{u} = \dot{\zeta}$, and

$$\begin{aligned}&\mathsf{M}_{11} = \begin{pmatrix}\mathcal{M}_{11} & 0\\ 0 & 1\end{pmatrix},\ \mathsf{A}_{11} = \begin{pmatrix}\mathcal{A}_{11} & 0\\ 0 & 0\end{pmatrix},\ \mathsf{A}_{12} = \begin{pmatrix}\mathcal{A}_{12}\\ 0\end{pmatrix},\\ &\mathsf{B}_1 = \begin{pmatrix}B_{h_1}\\ 1\end{pmatrix}, \mathsf{B}_\infty = \begin{pmatrix}\mathcal{B}_{\infty 1}\\ 0\end{pmatrix}, \mathsf{C}_1 = \begin{pmatrix}\mathsf{C}_1 & (-CA^{-1}B_1)\end{pmatrix}.\end{aligned} \tag{41}$$

## Refrences


**B**arbagallo, A., Sipp, D., Schmid, P.J., 2009. Closed-loop control of an open cavity flow using reduced-order models. J. FLUID MECH. 641, 1-50.

**B**arkley, D., 2006. Linear analysis of the cylinder wake mean flow . EUROPHYS. LETT. 75, no. 5, 750-756.

**B**enner, P., Li, J.R., Penzl, T., 2008. Numerical solution of large-scale Lyapunov equations, Riccati equations, and linear-quadratic optimal control problems. NUMER. LINEAR ALGEBR. 15 ,755-777.

**B**ernstein, D.S., Haddad, W.M., 1989. LQG control with an $H_\infty$ performance bound: A Riccati equation approach. IEEE TRANS. AUTOM. CONTR. 34, no. 3, 683-688.

**C**omsol Multiphysics, 2012. Version 4.3.

**D**atta, B. N., 2004. Numerical Methods for Linear Control Systems. Elsevier Academic Press.

**D**oyle, J., Francis, B., Tannenbaum, A., 1990. Feedback control Theory. Macmillan Publishing Co.

**D**oyle, J.C., Walls, J., Stein, G., 1982. Performance and robustness analysis for structured uncertainty. IEEE DECIS. CONTR. P. 629-636.

**D**oyle, J., Stein, G., 1979. Robustness with observers. IEEE TRANS. AUTOM. CONTR. AC-24, 607-611.

**F**arag, A., Werner, H. 2002. Robust $H_2$ controller design and tuning for the ACC benchmark problem and a real-time application. Proc. IFAC World Congress. Barcelona, Spain.

**F**eron, E., 1997. Analysis of robust H2 performance using multiplier theory. SIAM Journal Control Optim., 35, 160-177.

**H**einkenschloss, M., Sorensen, D.C., Sun, K., 2008. Balanced truncation model reduction for a class of descriptor systems with application to the Oseen equations. SIAM J. SCI. COMPUT. 30, no. 2, 1038-1063.

**J**ovanović, M., Bamieh, B., 2001. Modeling flow statistics using the linearized Navier-Stokes equations. IEEE DECIS. CONTR. P. Orlando, Florida USA, 4944-4949.
**L**auga, E., Bewley, T.R., 2004. Performance of a robust control strategy on a nonlinear model of spatially developing flows. J. FLUID MECH. 512, 343-374.
**L**auga, E., Bewley, T.R., 2002. Modern control of linear global instability in a cylinder wake model. INT. J. HEAT FLUID FL. 23, 671-677.
**L**ehoucq, B., Sorensen, D.C., Yang, C., 1998. Solution of large-scale eigenvalue problems with implicity restarted Arnoldi methods. ARPACK Users' Guide. SIAM.
**P**ackard, A., Doyle, J. 1987. Robust control with an $H_2$ performance objective. Proc. ACC. Minneapolis, 2141-2146.
**R**avanbod, L., Noll, D., Apkarian, P., 2012. An extension of the LQG-LTR procedure. IET CONTROL THEORY A. 6, no. 14, 851-866.
**R**aymond, J.P., Thevenet, L., 2010. Boundary feedback stabilization of the two dimensional Navier-Stokes equations with finite dimensional controllers. DISCRET CONT. DYN. S. 27, no. 3, 1159-1187.
**S**tein, G., Athans, M., 1987. The LQG-LTR Procedure for Multivariable Feedback Control Design. IEEE TRANS. AUTOM. CONTR. AC-32, 105-114.
**T**hevenet, L. 2009. Lois de feedback pour le contrôle d'écoulements. Thesis, Toulouse, Paul Sabatier University.
**V**arga, A., 1995. On stabilization methods of descriptor systems. SYST. CONTROL LETT. 24, no. 2, 133-138.
**V**arga, A., 1981, A Schur method for pole assignment. IEEE TRANS. AUTOM. CONTR. AC-26, 517-519.
**Z**hou, K., Doyle, J.C., 1998. Essentials of Robust Control. Prentice Hall.